Distance Measures of Autoregressive Models for Structural Damage Detection

Thesis by
Haitao Zheng

In Partial Fulfillment of the Requirements
for the Degree of

Doctor of Philosophy

Directed by
Professor Akira Mita

Keio University

March 2008

Abstract

The key to damage detection of civil engineering structures is to find an effective damage indicator. The damage indicator is expected to promptly detect the damage and accurately identify the damage state. For this purpose, a novel damage indicator defined as the distance measures of AR models was proposed.

The AR model has been successfully applied to parameterize the dynamical responses, typically the acceleration response. The premise of this approach is that the distance between the AR models, fitting the dynamical responses from the damaged and undamaged structures, may be correlated with the information of the damage, including the damage location and severity.

The distance measures of AR models have been widely used in speech recognition even if they are not known in civil engineering application. This research attempted to explore the feasibility of using the distance measures of AR modeling as the damage indicators. Two distance measures were considered as the damage indicators: one is the cepstral distance, and the other is the Itakura distance.

However, the current distance measures are limited to single-input single-output (SISO) models. In civil engineering, the structures are in general multi-input multi-output (MIMO) models. When dealing with the MIMO with mutually correlated excitations, the distance measures are able to detect the damage but not damage localization. To overcome the difficulty, the pre-whitening filter is introduced to remove the mutual correlations among the multiple outputs. Thus, we propose a damage detection methodology combining the distance measures of AR models and the pre-whitening filter.

To evaluate the proposed methodology, numerical and experimental data have been tested. The structure models for the evaluations are five storey models. In numerical evaluations, we consider different types of excitations, including mutually uncorrelated and correlated excitations. The damage scenarios are simulated by the different levels of inter-storey stiffness reduction, from 2% to 10%, and by the damages appearing on different storey. The measurement noises are also considered by adding measurement noises with 10% level to the acceleration outputs. In experimental evaluations, the damages scenarios include the cases of removing the columns and the braces. Results of the evaluations indicate that the distance measures of AR models are qualified for the damage indicators, and that the pre-whitening filters are crucial for the distance measures to carry out damage detection, especially for damage localization.

Acknowledgments

I would like to express my sincere gratitude to my advisor, Professor Akira Mita, for his kind concern, patient guidance and great encouragement throughout my time at Keio University. The continuous and open-minded discussions have been the sources of ideas, without which I could not fulfill this work.

Special thanks go to Professor Songtao Xue, my former advisor at Tongji University and Mr. Isamu Yokoi from Tokyo Sokushin Corporation for their valuable guidance and support.

Many thanks go to Professor Akira Sano, Professor Nozomu Hamada and Assistant Professor Masayuki Kohiyama for reviewing this thesis and giving me a wealth of precious advice.

Many thanks go to all the members of Mita laboratory for their warm friendship and memorial moments we shared, which make my graduate life happy and colorful.

Many thanks go to Keio University's Japanese Government (MEXT) Scholarship Program for the financial support during my graduate study.

Finally, I am deeply grateful to my parents, and my wife, Jinyi Tang, to whom this thesis is dedicated to, for their everlasting love.

Table of Contents

Chapter 1

Introduction

1.1 Current Damage Detection Methods

The civil engineering structures, such as buildings or bridges, begin to deteriorate once they are constructed and used. Damage can accumulate incrementally over long period of service time such as that associated with fatigue or corrosion damage accumulation. Damage can also result from extreme events such as an earthquake or blast loading (Sohn et al. 2003). With deteriorating structures increasing dramatically, the costs of maintenance become prohibitive and heavily bear on the country economics (De Roeck 2003). Damage detection is the process to inspect the structure and determine if the structure is safe and reliable. If the damaged is detected, the damage location and severity are further identified. Therefore, early and accurate damage detection can not only prevent catastrophic failures but also save costs for maintenance significantly.

Some traditional damage detection techniques using non-destructive evaluation (NDE), such as acoustic, magnetic and thermal field, radiography, and eddy current methods, have been developed. Such methods are primarily used for damage characterization and as a severity check, requiring a priori knowledge of the possible damage sites (Farrar et al. 2007). The NDE methods are ‘local’ damage detection methods, which is usually carried out in a local manner after the damage has been detected and located. Also the results obtained from NDE are often inconclusive and difficult to interpret. The NDE sensors can provide the possible damage by monitoring the changes in stress or strain states. However, it may be time consuming and too expensive to instrument all elements and components that are possibly critical, and access is not always possible (Chang et al. 2003, Humar et al. 2006).

As a comparably recent category of damage detection methods, the vibration-based methods have become most acceptable tools to determine the safety of structures. The premise of vibration-based damage detection approach is that the damage will significantly alter the measured dynamic response, due to changes in stiffness, mass or energy dissipation (Sohn et al. 2003). These methods are 'global' damage detection methods. Most vibration-based methods are concerned about finding shifts in modal frequencies, mode shapes, flexibility matrix, and shape curvature and so on (Doebling et al. 1998, Carden et al. 2004, Worden et al. 2004). These methods are often referred to as modes-based methods because of the damage indicators in the modal domain. The modes-based methods offer some advantages such as: no requirement of a prior of damage location information; no requirement of a mass of sensors; easy interpretation of modal parameters and so on. However, a major limitation associated with the modes-based methods is that the vibration characteristics, in modal domain, are global properties of the structure. As a result, it may be difficult for the global properties to identify the local damage unless the damage is very severe or the measurements are accurate at fairly high rate. Furthermore, the modes-based methods rely heavily on the physical or finite element model of structure, which is a time-consuming task, especially for a complex and large structure.

Within the broader family of vibration-based methods, time-series-based methods become another important category (Fassois et al. 2007). Such methods are data-based rather than physics-based, thus bringing an obvious advantage, that is, no physical or finite element models are required. The AR model, the most typical time series model, has been receiving attentions in damage detection field. The AR parameters have been treated as damage indicators to identify structural damage by some researchers. For examples: Worden et al. (2000) considered statistical process control approach to damage detection, using the mean and variance of the residuals of the AR model to form the statistical process control charts; A statistical pattern recognition methodology was presented by Sohn et al. (2001). The dynamic signals recorded were modeled using autoregressive (AR) time series models. By statistically examining changes in AR coefficients, they could classify signals from either undamaged or damaged systems; Fanning et al. (2001) used the mean and variance of the residuals of the AR model to form the statistical process control charts; Nair et al. (2006) proposed a sensitive damage indicator which only takes the first three AR coefficients of Auto-Regressive Moving-Average (ARMA) model; Mattson et al. (2006) chose the standard deviation of the residual of vector AR (VAR) model as the

damage indicator; De Lautour et al. (2006) used the AR coefficients as input features into an Artificial Neural Network (ANN). The damage and its extent were identified by observing the changes in AR coefficients. However, a disadvantage of these methods is that, without the benefits of pattern recognition tools, they can not provide information on damage localization or quantification.

1.2 Proposed Method

In this research, a novel damage indicator defined as distance measure between AR models is proposed. Most current time-series based damage detection methods are concerning about the changes in residuals of models, while the proposed method tries to find the changes in AR parameters by distance measures. The premise of this approach is that the distance between the AR models, fitting the dynamical responses from the damaged and undamaged structures, may be correlated with the information of the damage, including the damage location and severity. In this method, a baseline model is required to be compared with the structure to be inspected. In general, the newly-built or safety identified structure is referred to as the baseline state.

The distance measures of AR models have been widely used in speech recognition, such as the cepstral distance and the Itakura distance (Rabiner 1993, Chapter 4). We assume that the dynamical responses from the structure are recognized as the sound of the vibration structure. Based on this assumption, the application of distance measure to recognize the possible damaged civil engineering structure is explored in this research. However, the distance measures of AR models are proposed for the single-input single-output (SISO) models. The civil engineering structures are in general multiple-input multiple-output (MIMO) models with mutually correlated inputs. This results in the difficulty that the distance measures are not good for damage localization. To overcome this difficulty, a pre-whitening transform technique is introduced to remove the correlations among the structural responses.

The flowchart of the proposed damage detection method is shown in Figure 1.1. The procedure of the method is composed of the steps as follows:

- Firstly, the sensor signals, typically acceleration measured from each storey, are decorrelated to remove the mutual correlations by using the pre-whitening filter.
- Secondly, the uncorrelated signals are parameterized by AR modeling. The AR models are used to fit the vibration signals from the baseline structure and the structure to be identified.
- Thirdly, the damage indicator is defined as the distance measure between AR models. This distance measures can be obtained by either the cepstral distance or the Itakura distance.
- Finally, damage detection and localization are carried out based on the results of distance measures.

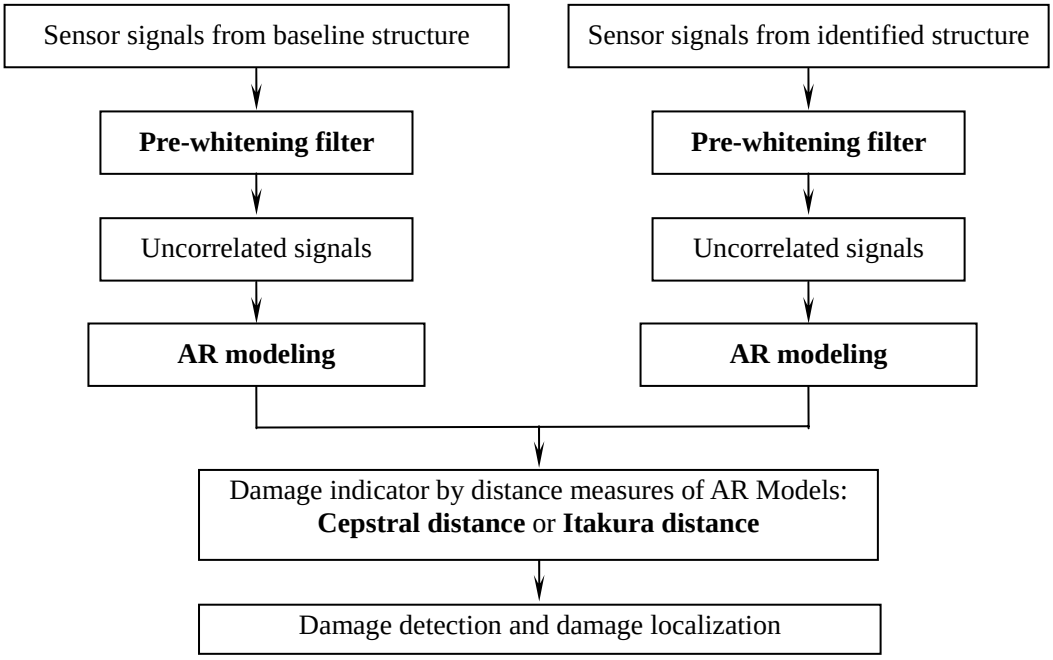

Figure 1.1: Flowchart of proposed damage detection method.

1.3 Overview of Thesis

The work in this thesis is divided into three parts. They are described in the three chapters respectively.

In Chapter 2, we first give an introduction of AR model, and present three model parameter estimation methods and four model order selection criteria. This chapter builds the basis for the study of damage detection using AR modeling. We evaluate the performances of various methods and criteria by the data samples of acceleration measurements.

Chapter 3 deals with the distance measures of AR model. Two distance measures, the cepstral distance and the Itakura distance, are introduced. We propose to use the distance measures as the damage indicators for damage detection of civil engineering structures. Numerical verifications show that the distance measures succeed in damage detection and localization without pre-whitening filter when dealing with the multiple mutually uncorrelated excitations, but fail in damage localization when dealing with the multiple mutually correlated excitations

Chapter 4 overcomes the difficulty encountered in Chapter 3 by introducing the pre-whitening filter. Before the AR modeling, the sensor signals are passed through the pre-whitening filter to remove the mutual correlations. The proposed damage detection method combines the distance measures with the pre-whitening filters. Numerical and experimental evaluations show how the pre-whitening filters improve the identifying ability of damage location of distance measures.

Finally in Chapter 5, we give a conclusion remark of our work and list the limitations and unresolved problems.

Chapter 2

Autoregressive Model

In this chapter, we give insight into the properties of autoregressive model and the parameter estimation methods and the model order selection criteria. In Section 2.1, we first present an overview of the basics of three classes of parametric models of linear time invariant dynamic system: autoregressive (AR) models, moving average (MA) models and mixed autoregressive/moving average (ARMA) models. In the ARMA class models, we will particularly discuss about the AR signals, which are most frequently used in applications. The process of fitting the parametric model involves two separate stages, namely:

1. The estimation of parameters of the model;
2. The determination of order of the model.

Then, in Section 2.2, we introduce three widely used methods of extracting the AR model parameters from a given measured signal values. These methods are:

1. The Yule-Walker method;
2. The Least Squares method;
3. The Burg's method.

In Section 2.3, we discuss about how to determine the model order, which is a crucial important issue of AR modeling. Four famous model selection criteria are introduced:

1. The Final Prediction Error Criterion (FPE);
2. The Akaike Information Criterion (AIC);
3. The Bayesian AIC (BIC);
4. The Schwarz Bayesian Criterion (SBC).

For application in SHM, we focus on the AR modeling of dynamical responses from structures, for example the acceleration time series. In Section 2.4 we show the performances of the above various methods and criteria on the data samples, which were measured from a shake table test of five-storey building model.

Introduction of Autoregressive Model

In this section, we describe three classes of parametric single-input-single-output (SISO) models: ARMA model, MA model and AR model. A few properties for the three models are given.

The parametric methods are based on modeling the data sequence $x(n)$ as the output of a linear discrete-time system, which is characterized by a rational or system function in the z-domain:

$$H(z)=\frac{B(z)}{A(z)}=\frac{\sum_{j=0}^{q} b(j)z^{-j}}{1+\sum_{i=1}^{p} a(i)z^{-i}} \tag{2.1.1}$$

2.1.1 ARMA Model

The above linear discrete-time system can also be described by a linear constant-coefficient difference equation as follows

$$x(n)+\sum_{i=1}^{p} a(i)x(n-i)=\sum_{j=0}^{q} b(j)e(n-j) \tag{2.1.2}$$

where $e(n)$ is the input sequence to the system, assumed to be white noise of variance equal to σ^2. This expression is called an autoregressive moving average (ARMA) process of order (p,q), and it is usually denoted as $ARMA(p,q)$. The $a(i)$ constitute the AR part and the $b(i)$ the MA part of the model, and they are referred to as the AR parameters and MA parameters.

The zeros of rational function $H(z)$ are the values of z for which $H(z)=0$. The poles of rational function $H(z)$ are the values of z for which $H(z)=\infty$. Since $B(z)$ and $A(z)$ are polynomials in the z-domain, they can be expressed in factored form as

$$\begin{aligned} H(z) &= \frac{B(z)}{A(z)} = b(0)z^{-q+p}\,\frac{(z-\beta(1))(z-\beta(2))\cdots(z-\beta(q))}{(z-\alpha(1))(z-\alpha(2))\cdots(z-\alpha(p))} \\ &= b(0)z^{-q+p}\,\frac{\prod_{j=1}^{q}(z-\beta(j))}{\prod_{i=1}^{p}(z-\alpha(i))} \end{aligned} \tag{2.1.3}$$

Thus, the rational system function $H(z)$ has q finite zeros at $z=\beta(1),\beta(2),\cdots,\beta(q)$ (the roots of the numerator polynomial), p finite poles at $z=\alpha(1),\alpha(2),\cdots,\alpha(q)$ (the roots of the denominator polynomial), and $|p-q|$ zeros (if $p<q$) or poles (if $p<q$) at the origin $z=0$.

2.1.2 MA Model

The second possible model is obtained by setting $A(z)=1$, so that the rational system function reduces to

$$H(z)=B(z)=\sum_{j=0}^{q}b(j)z^{-j} \tag{2.1.4}$$

Then (2.1.2) becomes

$$x(n)=\sum_{j=0}^{q}b(j)e(n-j), \tag{2.1.5}$$

which is called a moving average (MA) process of order q and denoted as $MA(q)$. In this case, $H(z)$ consists of q zeros, whose values are determined by the MA parameters $b(j)$, i.e. the roots of the polynomial $B(z)$.

Since the system function in (2.1.4) contains only nontrivial zeros and the corresponding system is also called an all-zero system.

2.1.3 AR Model

If $q = 0$ and $b(0) = 1$, the resulting rational system function of the model reduce to

$$H(z) = \frac{1}{A(z)} = \frac{1}{1 + \sum_{i=1}^{p} a(i) z^{-i}} \tag{2.1.6}$$

Then (2.1.2) becomes

$$x(n) + \sum_{i=1}^{p} a(i) x(n-i) = e(n), \tag{2.1.7}$$

which is called an autoregressive (AR) process of order p, or denoted as $AR(p)$. In this case, $H(z)$ consists of p poles, whose values are determined by the AR parameters $a(i)$, i.e. the roots of the polynomial $A(z)$.

Since the system function in (2.1.4) contains only nontrivial poles and the corresponding system is also called an all-pole system. If the poles lie inside the unit circle, the AR model is guaranteed to be stable.

Brief Forms Using Delay Operator

By using the filter delay operator q^{-1} ($q^{-k} x(n) = x(n-k)$), the system function (2.1.1) can be written as

$$H(q) = \frac{B(q)}{A(q)}, \tag{2.1.8}$$

The corresponding difference equation becomes

$$A(q) x(n) = B(q) e(n) \tag{2.1.9}$$

Hence, the three parameter models are summarized in brief forms as below:

$$\begin{aligned} &ARMA \quad Model: && A(q)x(n) = B(q)e(n) \\ &MA \quad Model: && x(n) = B(q)e(n) \\ &AR \quad Model: && A(q)x(n) = e(n) \end{aligned} \tag{2.1.10}$$

Of the three linear models the AR model is by far the most widely used. The reasons are twofold.

1. The AR model is suitable for representing spectra with narrow peaks (resonance). This is an important feature since narrowband spectra are quite common in practice.

2. The AR model results in very simple linear equations for the AR parameters. The estimation of AR parameters is a well-established topic and the stability of the estimated AR polynomial can be guaranteed.

Model Parameter Estimation

In this section, we are concerned with the estimation of the AR model parameters. The study on model parameter estimation for the ARMA classic models has a relatively long history. For a historical perspective, we referred to the related books by Priestley (1994), Stoica et al. (1997), Proakis et al. (2006) and others.

Yule-Walker Method

The Yule-Walker method for estimating the AR parameters is based on the Yule-Walker equation consisting of covariance elements, which are replaced by the sample covariances in practical parameter estimation process (Yule 1927, Walker 1931). Before introducing the Yule-Walker method, let's examine the covariance structure of ARMA process since almost all the parameter estimation methods exploit this covariance structure. The expression provides a convenient method for estimating the ARMA parameters by replacing the true autocovariances with estimates obtained

from data.

(2.1.2) can be written as

$$x(n)+\sum_{i=1}^{p}a(i)x(n-i)=\sum_{j=0}^{q}b(j)e(n-j),\qquad (b(0)=1) \tag{2.2.1}$$

Multiplying the above expression by $x^*(n-k)$ and taking expectation yields

$$r(k)+\sum_{i=1}^{p}a(i)r(k-i)=\sum_{j=0}^{q}b(j)E\{e(n-j)x^*(n-k)\} \tag{2.2.2}$$

Hereafter, the symbol $(\cdot)^*$ denotes the conjugate transpose of a vector and $E\{\cdot\}$ the expectation operator (which averages over the ensemble of realizations). In (2.2.2), $r(k)$ is the autocovariance sequence of output signal $x(n)$, defined as

$$r(k)=E\{x(n)x^*(n-k)\} \tag{2.2.3}$$

Since the system function $H(q)$ is asymptotically and casual, we have

$$H(q)=\frac{B(q)}{A(q)}=\sum_{k=0}^{\infty}h_k q^{-k},\qquad (h_0=1). \tag{2.2.4}$$

Then, the input $e(n)$ to the system and the corresponding output $x(n)$ are related via the convolution sum

$$x(n)=H(q)e(n)=\sum_{k=0}^{\infty}h_k e(n-k) \tag{2.2.5}$$

The term $E\{e(n-j)x^*(n-k)\}$ becomes

$$\begin{aligned}E\{e(n-j)x^*(n-k)\}&=E\left\{e(n-j)\sum_{s=0}^{\infty}h_s^*e^*(n-k-s)\right\}\\&=\sigma^2\sum_{s=0}^{\infty}h_s^*\delta_{j,k+s}=\sigma^2h_{j-k}^*\end{aligned} \tag{2.2.6}$$

where the Kronecker delta $\delta_{j,k+s}$ satisfies: $\delta_{j,k+s}=0$ if $j=k+s$, otherwise $\delta_{j,k+s}=0$.

Considering the convention that $h_k = 0$ for $k < 0$, (2.2.2) becomes

$$r(k) + \sum_{i=1}^{p} a(i) r(k-i) = \sigma^2 \sum_{j=0}^{q} b(j) h^*_{j-k} \tag{2.2.7}$$

When $k > m$, the above equation reduces to

$$r(k) + \sum_{i=1}^{p} a(i) r(k-i) = 0, \qquad k > m \tag{2.2.8}$$

Hence, for AR process, since $m = 0$, (2.2.8) holds for $k > 0$. Thus for $k = 0$, from (2.2.7) we have

$$r(0) + \sum_{i=1}^{p} a(i) r(-i) = \sigma^2 \sum_{j=0}^{q} b(j) h^*_j = \sigma^2 \tag{2.2.9}$$

Combining (2.2.8) and (2.2.9) for $k = 1,2,\cdots,p$ gives the following system of linear equations

$$\begin{bmatrix} r(0) & r(-1) & \cdots & r(-p) \\ r(1) & r(0) & \cdots & r(-p+1) \\ \vdots & \vdots & \ddots & \vdots \\ r(p) & r(p-1) & \cdots & r(0) \end{bmatrix} \begin{bmatrix} 1 \\ a(1) \\ \vdots \\ a(p) \end{bmatrix} = \begin{bmatrix} \sigma^2 \\ 0 \\ \vdots \\ 0 \end{bmatrix} \tag{2.2.10}$$

The above equations are called the Yule-Walker equations, which are basis of many AR parameter estimation methods.

If $\{r(k)_{k=0}^{p}\}$ were known, solving (2.2.10) gives the parameters for AR process of order p

$$\theta = [a(1), a(2), \cdots, a(p)]^T \tag{2.2.11}$$

Hereafter, $(\cdot)^T$ denotes transpose of a vector or matrix.

Then, by using all but the first row of (2.2.10)

$$\begin{bmatrix} r(1) \\ \vdots \\ r(p) \end{bmatrix} + \begin{bmatrix} r(0) & \cdots & r(-p+1) \\ \vdots & \ddots & \vdots \\ r(p-1) & \cdots & r(0) \end{bmatrix} \begin{bmatrix} a(1) \\ \vdots \\ a(p) \end{bmatrix} = \begin{bmatrix} 0 \\ \vdots \\ 0 \end{bmatrix} \tag{2.2.12}$$

or, written in brief

$$r + R\theta = 0 \tag{2.2.13}$$

where $r = [r(1), r(2), \cdots, r(p)]^T$ and the covariance matrix of output signal $x(n)$

$$\begin{aligned} R &= \begin{bmatrix} r(0) & \cdots & r(-p+1) \\ \vdots & \ddots & \vdots \\ r(p-1) & \cdots & r(0) \end{bmatrix} \\ &= E\left\{ \begin{bmatrix} x^*(n-1) \\ x^*(n-2) \\ \vdots \\ x^*(n-p) \end{bmatrix} \begin{bmatrix} x(n-1) & x(n-2) & \cdots & x(n-p) \end{bmatrix} \right\} \end{aligned} \tag{2.2.14}$$

The solution of the above equations is

$$\theta = -R^{-1} r \tag{2.2.15}$$

For the available signal samples $\{x(1), \cdots x(N)\}$, the estimate of the covariance lag $r(k)$ can be obtained. There are two standard means to obtain the sample covariance:

$$\hat{r}(k) = \frac{1}{N-k} \sum_{n=k+1}^{N} x(n) x^*(n-k) \qquad 0 \le k \le N-1 \tag{2.2.16}$$

and

$$\hat{r}(k) = \frac{1}{N} \sum_{n=k+1}^{N} x(n) x^*(n-k) \qquad 0 \le k \le N-1 \tag{2.2.17}$$

The first estimator is called standard unbiased autocovariance sequence, and the second one standard biased autocovariance sequence. In common, the latter one is

most commonly used since that the estimate covariance matrix $\hat{R}$ obtained from the biased autocovariance sequence $\{\hat{r}(k), k \geq 0\}$ is guaranteed to be positive definite.

By inserting the sample covariances $\{\hat{r}(k)\}_{k=0}^{p}$ into and solving (2.2.12) gives the estimates of AR parameters $\hat{\theta}$. Since the estimate of covariance matrix $\hat{R}$ is positive definite, the solution to (2.2.12) $\hat{\theta}$ is unique. Once $\hat{\theta}$ is known, the estimate of input variance $\hat{\sigma}^2$ can be obtained from the first row of (2.2.10).

Least Squares Method

The least squares method of AR parameter estimation is based on a least squares minimization criterion which minimizes the prediction error variance. The least squares AR model uses the time-domain relation $A(q)x(n) = e(n)$. The least squares estimator is developed by considering the closely related problem of linear prediction.

Firstly, let's relate the Yule-Walker equations to the linear prediction problem. Assume $x(n)$ be an AR process of order p. Rewriting (2.1.7) gives

$$\begin{aligned} e(n) &= x(n) + \sum_{i=1}^{p} a(i)x(n-i) = x(n) + \varphi^T(n)\theta \\ &\stackrel{\Delta}{=} x(n) + \hat{x}(n) \end{aligned} \tag{2.2.18}$$

where $\varphi^T(n) = [x(n-1), \cdots x(n-p)]^T$.

$\hat{x}(n)$ is interpreted as a linear prediction of $x(n)$ from the p previous samples $x(n-1), \cdots, x(n-p)$. $e(n)$ is interpreted as the corresponding prediction error.

Then the AR parameter vector θ is estimated by minimizing the prediction error variance

$$\sigma_p^2 \stackrel{\Delta}{=} E\left\{|e(n)|^2\right\} \tag{2.2.19}$$

Combining (2.2.17) and (2.2.19) gives

$$\begin{aligned}\sigma_p^2 \overset{\Delta}{=} E\left\{e(n)^2\right\} &= E\left\{\left[x^*(n)+\theta^*\varphi^c(n)\right]\left[x(n)+\varphi^T(n)\theta\right]\right\} \\ &= r(0)+r^*\theta+\theta^*r+\theta^*R\theta\end{aligned} \tag{2.2.20}$$

where r and R have been defined in (2.2.13) and (2.2.14). The symbol $(\cdot)^*$ denotes the conjugate transpose of a vector or matrix and the symbol $(\cdot)^c$ denotes the conjugate of a vector or matrix. The AR parameter vector θ that minimizes (2.2.20) is given by

$$\theta = -R^{-1}r \tag{2.2.21}$$

and the minimum prediction error

$$\sigma_p^2 = r(0) - r^*R^{-1}r \tag{2.2.22}$$

It can be found that (2.2.20) and (2.2.21) are exactly the Yule-Walker equations in (2.2.10). The Yule-Walker equations can therefore be interpreted as the solution to the problem of finding the best linear predictor of $x(n)$ from its p most recent past samples. For this reason, AR modeling is sometimes referred to as linear predictive modeling.

The least square AR parameter estimation method is based on a finite-sample approximate solution of the above minimization problem. For the available signal samples $\{x(1),\cdots x(N)\}$, the minimization of the prediction error variance $E\left\{e(n)\right|^2\}$ is approximated by the finite sample cost function

$$\begin{aligned}f(\theta) &= \sum_{n=N_1}^{N_2}\left|e(n)\right|^2 = \sum_{n=N_1}^{N_2}\left|x(n)+\sum_{i=1}^{p}a(i)x(n-i)\right|^2 \\ &= \left\|\begin{bmatrix} x(N_1) \\ x(N_1+1) \\ \vdots \\ x(N_2)\end{bmatrix} + \begin{bmatrix} x(N_1-1) & x(N_1-2) & \cdots & x(N_1-p) \\ x(N_1) & x(N_1-1) & \cdots & x(N_1-p+1) \\ \vdots & \vdots & \ddots & \vdots \\ x(N_2-1) & x(N_2-2) & \cdots & x(N_2-p)\end{bmatrix}\theta\right\|^2 \\ &\overset{\Delta}{=} \left\|x+X\theta\right\|^2\end{aligned} \tag{2.2.23}$$

where we assume

$$x(n) = 0, \qquad n < 1; \quad n > N \tag{2.2.24}$$

The estimate of AR parameter vector θ that minimizes the cost function $f(\theta)$ is given by

$$\hat{\theta} = -(X^* X)^{-1}(X^* x) \tag{2.2.25}$$

The definition of x and X in (2.2.24) depend on the choices of N_1 and N_2. For example, for $N_1 = 1$ and $N_2 = N + p$, x and X become

$$x = \begin{bmatrix} x(1) \\ x(2) \\ \vdots \\ \hline x(p+1) \\ x(p+2) \\ \vdots \\ \underline{x(N)} \\ 0 \\ 0 \\ \vdots \\ 0 \end{bmatrix}, \qquad X = \begin{bmatrix} 0 & 0 & \cdots & 0 \\ x(1) & 0 & \cdots & 0 \\ \vdots & \vdots & \ddots & \vdots \\ \hline x(p) & x(p-1) & \cdots & x(1) \\ x(p+1) & x(p) & \cdots & x(2) \\ \vdots & \vdots & \ddots & \vdots \\ \underline{x(N-1)} & \underline{x(N-2)} & \cdots & \underline{x(N-p)} \\ x(N) & x(N-1) & \cdots & x(N-p+1) \\ 0 & x(N) & \cdots & x(N-p+2) \\ \vdots & \vdots & \ddots & \vdots \\ 0 & \cdots & 0 & x(N) \end{bmatrix} \tag{2.2.26}$$

Notice the Toeplitz structure of X, and note that x matches this Toeplitz structure when it is appended to the left of X; that is, $[x|X]$ also shares the Toeplitz structure.

The two most common choices for N_1 and N_2 are:

1. $N_1 = 1$ and $N_2 = N + p$, as shown above. This choice yields the so-called autocorrelation method.

2. $N_1 = p + 1$ and $N_2 = N$. This choice corresponds to removing the first p and last p rows of x and X in (2.2.26). Hence, all the arbitrary zero values are eliminated. This choice yields the so-called covariance method. This method is called the covariance least squares method, or the least squares method.

Other choices have also been suggested. For example, the prewindow method uses $N_1 = 1$ and $N_2 = N$; and the postwindow method uses $N_1 = p + 1$ and $N_2 = N + p$.

The least squares methods can be interpreted as approximate solutions to the Yule-Walker equations in (2.2.12) by recognizing that X^*X and X^*x are, to within a multiplicative constant, finite-sample estimates of R and r , respectively. In fact, it is easy to show that for the autocorrelation method, the elements of $\frac{(X^*X)}{N}$ and $\frac{(X^*x)}{N}$ are exactly the biased autocovariance sequence estimates (2.2.17), which is used in the Yule-Walker AR parameter estimation method.

$$\hat{\theta} = -\left[\frac{1}{N}(X^*X)\right]^{-1}\left[\frac{1}{N}(X^*x)\right] \tag{2.2.27}$$

Hence, a consequence can be found that: the autocorrelation of least squares method is equivalent to the Yule-Walker method.

For small or medium sample lengths, the Yule-Walker and covariance least squares methods may behave differently. The least square model has been found to be more accurate than the Yule-Walker method. That is, the estimated AR parameters of the former are on the average closer to the true values than those of the latter.

The theoretical explanation of this behavior is not possible since the finite-sample statistical analysis of these methods is underdeveloped. A heuristic explanation is the assumption that, for the autocorrelation method of least squares method (the Yule-Walker method), the signal samples $x(n) = 0$ outside of the interval $1 \le n \le N$. Hence, $\frac{(X^*X)}{N}$ and $\frac{(X^*x)}{N}$ are biased estimates of R and r in (2.2.12) and (2.2.13), which results in the bias in Yule-Walker estimated of the AR parameter. Whereas, for the covariance least squares method, any measurement data outside the available interval $1 \le n \le N$ are not used, hence $\frac{(X^*X)}{N-p}$ and $\frac{(X^*x)}{N-p}$ are unbiased estimates of R and r in (2.2.12) and (2.2.13).

On the other hand, The Yule-Walker method is always guaranteed to be stable, while the least squares method may be unstable. Stability of the model is often an important

requirement. The lack of guaranteed stability is a drawback of the least squares method. However, the case is that the AR model estimated by least square method is unstable only infrequently.

For large sample length, the difference between the covariance matrix estimates used by the Yule-Walker method and least squares method diminishes. Consequently, the Yule-Walker and least squares estimates of AR parameters nearly coincide with each other when considering a long AR process.

Burg's Method

The Burg's method is based on forward and backward prediction errors, and on estimation of the reflection coefficients. This method was developed by Burg (1975). Assume we have the data measurements $x(n)$ for $n = 1,2,\cdots N$. Then we define the forward and backward prediction errors for a p order AR model as

$$\hat{e}_{f,p}(n) = x(n) + \sum_{i=1}^{p} \hat{a}_p(i) x(n-i), \qquad n = p+1,\cdots,N \tag{2.2.28}$$

$$\hat{e}_{b,p}(n) = x(n-p) + \sum_{i=1}^{p} \hat{a}_p^*(i) x(n-p+i), \qquad n = p+1,\cdots,N \tag{2.2.29}$$

where the hats used in the equations denoted estimated quantities, and we explicitly denote the order p in both the prediction error sequences and the AR parameters. The AR parameters are related to the reflection coefficients $\hat{k}_p$ by

$$\hat{a}(i) = \begin{cases} \hat{a}_{p-1}(i) + \hat{k}_p \hat{a}_{p-1}^*(p-i), & i = 1,\cdots,p-1 \\ \hat{k}_p, & i = p \end{cases} \tag{2.2.30}$$

The Burg's method considers the recursive-in-order estimation of $\hat{k}_p$ given that the AR parameters for order $p-1$ have been computed. In practice, the Burg's method finds $\hat{k}_p$ to minimize the arithmetic mean of the forward and backward prediction error variance estimates:

$$\min_{\hat{k}_p} = \frac{1}{2}\left[\hat{r}_f(p) + \hat{r}_b(p)\right] \tag{2.2.31}$$

where

$$\hat{r}_f(p) = \frac{1}{N-p}\sum_{n=p+1}^{N}\left|\hat{e}_{f,p}(n)\right|^2 \tag{2.2.32}$$

$$\hat{r}_b(p) = \frac{1}{N-p}\sum_{n=p+1}^{N}\left|\hat{e}_{b,p}(n)\right|^2 \tag{2.2.33}$$

and where $\left\{\hat{a}_{p-1}(i)\right\}_{i=1}^{p-1}$ are assumed to be known form the recursion at the previous order.

Show that the prediction errors satisfy the following recursive-in-order expressions

$$\hat{e}_{f,p}(n) = \hat{e}_{f,p-1}(n) + \hat{k}_p\hat{e}_{b,p-1}(n-1) \tag{2.2.34}$$

$$\hat{e}_{b,p}(n) = \hat{e}_{b,p-1}(n-1) + \hat{k}_p^*\hat{e}_{f,p-1}(n) \tag{2.2.35}$$

Combining the above (2.2.34) with (2.2.35), and developing a recursive-in-order algorithm for estimating the AR parameters, the reflection coefficient is given by

$$\hat{k}_p = \frac{-2\sum_{n=p+1}^{N}\hat{e}_{f,p-1}(n)\hat{e}_{b,p-1}^*(n-1)}{\sum_{n=p+1}^{N}\left[\left|\hat{e}_{f,p-1}(n)\right|^2 + \left|\hat{e}_{b,p-1}(n-1)\right|^2\right]}, \tag{2.2.36}$$

which minimize (2.2.31).

A recursive-in-order algorithm for estimating the AR parameters is as follows:

1. Initialize $\hat{e}_{f,0}(n) = \hat{e}_{b,0}(n) = x(n)$;
2. Compute $\hat{e}_{f,p-1}(n)$ and $\hat{e}_{b,p-1}(n)$ for $n = p+1, \cdots, N$ from (2.2.34) and (2.2.35);
3. Compute $\hat{k}_p$ from (2.2.36);
4. Compute $\hat{a}_p(n)$ for $n = 1, \cdots, p$ from (2.2.30).

The vector of AR parameters can then be obtained by $\hat{\theta} = \left[\hat{a}_p(1), \cdots, \hat{a}_p(p)\right]^T$.

The Burg's method of AR model estimation is guaranteed to be stable. In addition, the Burg algorithm is computationally simple. On the other hand, the burg method is suboptimal in that it estimates the p reflection coefficients by decoupling an p -dimensional minimization problem into the p one-dimensional minimizations in (2.2.31). This is in contrast to the least squares method, in which the AR parameters are found by an p -dimensional minimization.

For large sample length, the three AR model estimation methods give very similar performance. For short or medium sample length, the Burg's method usually behaves somewhere between the Yule-Walker method and the least square method.

Model Order Selection

A very important issue of the use of the AR model is the selection of the model order p (Proakis and Manolakis, 2006). In the preceding sections we have discussed the problem of parameter estimation on the assumption that the orders of the AR operators were known a priori. In practice, the orders of these operators are almost invariably unknown. And the model orders constitute, in effect, additional unknown parameters for which suitable values have to be inferred from the data. As a general rule, if we select a model with too low an order, we obtain a highly smoothed spectrum. On the other hand, if the order is selected too high, we run the risk of introducing spurious low-level peaks in the spectrum.

We mentioned previously that one indication of the performance of the AR model fitting is the variance of the prediction error. The error variance is, in general, is different for each of the estimators described above. The characteristic of this prediction error is that it decreases as the order of the AR model is increased. We can decide the model order, by monitoring the rate of decrease and deciding to terminate the process when the rate of decease becomes relatively slow. However, it is apparent that this approach may be imprecise and ill defined.

Many theoretical discussions and experimental results on the model order selection have been given in literature [e.g., the papers by Gersch and Sharpe 1973, Ulrych and Bishop 1975, Tong 1975 and 1977, Jones 1976, Nuttall 1976, Berryman 1978, Kashyap 1980, Pukkila 1988 and Rezek et al. 1997, the books by Orfanidis 1985, Marple 1987, Wei 1990, Priestley 1994, Proakis and Manolakis 2006]. However, there is no definite result for the different model order selection criteria. In the absence of any prior information regarding the physical process that resulted in the data, it is apparent that one should try different model orders and different criteria. We now describe some widely used techniques of determining the order of AR model.

Two most famous criteria for selecting the model order have been developed by Akaike (1969, 1974). With the first, called the Final Prediction Error (FPE) criterion, the order is selected to minimize the performance indicator

$$FPE(p) = \frac{N+p}{N-p}\hat{\sigma}_p^2 \tag{2.3.1}$$

where N is the number of observations to which the model is fitted, and $\hat{\sigma}_p^2$ the estimated variance of the linear prediction error. Using this criterion, the fitting AR model has the property that it leads to the estimated one step prediction with the smallest mean square error. If we plot $FPE(p)$ against p the graph will, in general, show a definite minimum value at a particular value of p at which the FPE attains its minimum value as the appropriate order of the model.

The second criterion proposed by Akaike (1974) is called Akaike Information Criterion (AIC). This very general criterion, which is based on information theoretic concepts, can be used for statistical model identification in a wide range of situations and is not restricted to the time series context. When a model involving p independently adjusted parameters is fitted to data, the AIC is defined by

$$AIC(p) = N \ln \hat{\sigma}_p^2 + 2p \tag{2.3.2}$$

Note that the term $\hat{\sigma}_p^2$ decreases and therefore $\ln \hat{\sigma}_p^2$ also decreases as the order of the AR model is increased. However, $2p$ increases with an increase of order p. Hence, a minimum value can be obtained. If we plot $AIC(p)$ against p the graph will, in

general, show a definite minimum value, and the appropriate order of the model is determined by that value of p at which $AIC(p)$ attains its minimum value.

There is an asymptotically equivalent relationship between AIC and FPE. For large data length N,

$$\begin{aligned}\ln[FPE(p)] &= \ln\left[\frac{\left(1+\frac{p}{N}\right)}{\left(1-\frac{p}{N}\right)}\hat{\sigma}_p^2\right] \\ &= \ln\left(1+\frac{p}{N}\right)-\ln\left(1-\frac{p}{N}\right)+\ln\hat{\sigma}_p^2, \\ &\approx \ln\hat{\sigma}_p^2+\frac{2p}{N}\end{aligned} \tag{2.3.3}$$

Hence, we have

$$AIC(p) \approx N\ln[FPE(p)] \tag{2.3.4}$$

The AIC criterion has largely replaced the FPE criterion, and is now generally accepted as one of the most reliable methods for order determination. It has been widely applied to both simulated and real data with very successful results and has become a firmly established tool in time series model fitting.

In addition, there are some alternative criteria. Akaike (1979) has developed a new order determination criterion, called Bayesian Information Criterion (BIC), which is derived from a Bayesian modification of the AIC criterion. For a model involving p parameters fitted to observations $x(n)$ for $1 \le n \le N$, the BIC criterion takes the form

$$BIC(p) = N\ln\hat{\sigma}_p^2 - (N-p)\ln(1-(p)N) + p\ln N + p\ln\left[p^{-1}\left(\frac{\hat{\sigma}_X^2}{\hat{\sigma}_p^2}-1\right)\right] \tag{2.3.5}$$

where, $\hat{\sigma}_X^2$ is the variance of raw sample from the observations, while $\hat{\sigma}_p^2$ is the variance of estimated prediction error. When p is small relative to N we may use the approximation $-(N-p)\ln(1-(p)N) \to p$, so that

$$BIC(p) \approx AIC(p) + p(\ln N - 1) + p \ln\left[p^{-1}\left(\frac{\hat{\sigma}_X^2}{\hat{\sigma}_p^2} - 1 \right)\right] \tag{2.3.6}$$

Hence, the difference between BIC and AIC has the effect of increasing the weigh attached to the "penalty term", which take account of the number of AR parameters. Consequently, the minimization of BIC criterion generally leads to lower orders than those obtained by minimizing AIC. Shibata (1976) shown that when the true model is $AR(p_0)$, the estimate $\hat{p}$ derived from the AIC criterion is not a consistent estimate of p_0, but rather tends to overestimate p_0. On the other hand, the estimate obtained form the BIC criterion may well underestimate the true order.

Schwarz (1978) suggested a Bayesian criterion, called Schwarz Bayesian Criterion (SBC), is defined as

$$SBC(p) = N \ln \hat{\sigma}_p^2 + p \ln N \tag{2.3.7}$$

The SBC criterion is similar to Akaike's BIC in terms of its dependence on $\ln N$. In fact, if we use the above approximate for BIC, we may have

$$BIC(p) \approx SBC(p) + p\left\{ \ln\left[p^{-1}\left(\frac{\hat{\sigma}_X^2}{\hat{\sigma}_p^2} - 1 \right)\right] - 1 \right\} \tag{2.3.8}$$

Note that the Minimum Description Length criterion (MDL) (Rissanen, 1978, 1983) is also given by (2.3.7).

Kashyap (1980) showed that the AIC criterion tends is statistically inconsistent at $N \to \infty$, while the SBC criterion is statistically consistent. Lutkepohl [1985] compared SBC criterion with other order selection criteria in a simulation study and found that SBC chose the correct model order most often and led, on the average, to the smallest mean-squared prediction error of the fitted AR models. Some experiment results indicate that for small sample lengths, the order of the AR model should be selected to be in the range $N/3$ to $N/2$ for good results.

Illustration Examples

The comparison researches have indicated that the definitive results can not be yielded, either by the AR parameters estimation algorithms or by the model order selection criterion methods (the papers by Wear et al. 1995, De Hoon et al. 1996 and Schlogl 2006; the books by brockwell et al. 1991, Priestley 1994, Wei 1994, Ljung 1999, Stoica et al. 1997 and Proakis et al. 2006). For different physical process and sample length, the various methods may behave differently. Hence, different parameter estimate methods with different model order and various order selection criterion should be tried and compared.

In this section, we will evaluate the above various parameter estimation methods and model order selection criteria on the data samples of acceleration outputs measured from a shake table test (Building Research Institute of Japan, 2004). The experiments using the steel model were carried out under the US-Japan cooperative structural research project on Smart Structure Systems. The test structure model is a five-storey steel structure, depicted in Figure 2.1 (a). The structural model can be simplified as a five degree-of-freedom (DOF) system. Figure 2.1 (b) shows the five-DOF system, which is composed of five mass.

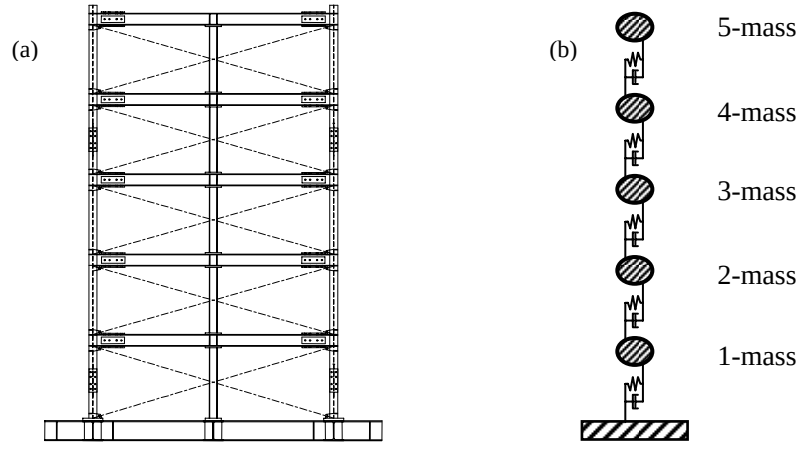

Figure 2.1: Experimental building model and its simplified model.

The weight of every storey is 2.57 ton and storey heights are all 1 m. The length of long-side is 3 m, while that of the short-side is 2 m. The excitation of test is a white noise with bandwidth of 0~200 Hz generated by the vibration exciter, along the long-side direction. On every storey of structure the accelerometers were mounted on both long-sides to record the acceleration responses along the long-side direction. The

acceleration time histories were recorded with the sampling period 0.005 second, for 40.92 seconds sensor signal records. Thus each acceleration record has 8,192 sampled data, shown in Figure 2.2.

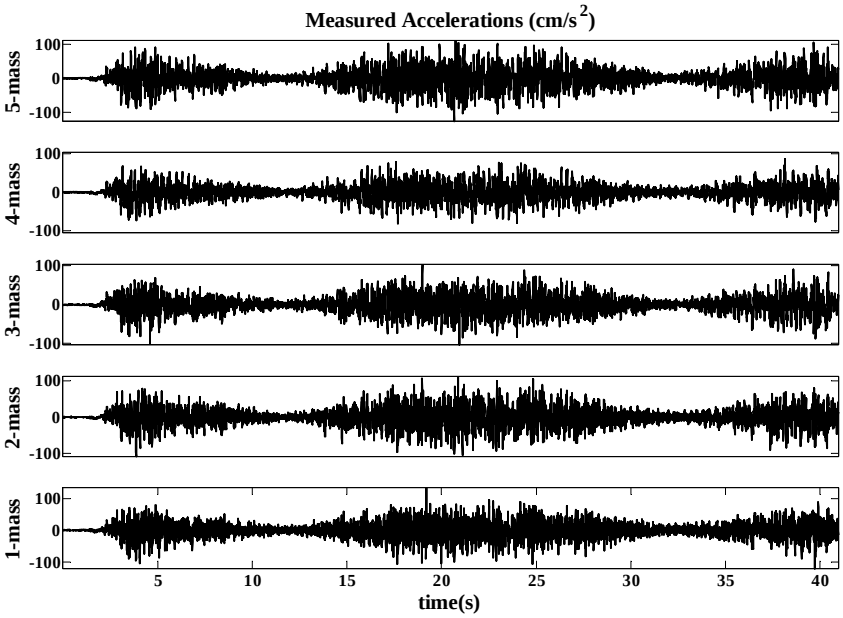

Figure 2.2: Acceleration outputs measured from building model.

It should be noted that various simulations for each mass have been conducted, not only in the analysis of parameter estimation but also that of order selection, almost all the results of different masses are the same. Therefore, we only give the results from the fifth mass in the following examples.

2.4.1 Parameter Estimation

Firstly, we discuss the AR modeling of the acceleration data samples by using three parameter estimation methods respectively: the Yule-Walker Method, the Least Squares Method and the Burg's method. To evaluate the stability of AR model, we will give the graphical interpretations of polar plots of system's poles for each method. The effect of different data length on AR parameter estimation is also discussed. We use three data lengths, which are 51, 201 and 501 data samples. Although the classification of data length has not been defined yet, the selections of data length in this study are similar to the paper by Schlogl (2006).

Data length of 51

Figure 2.3 shows the consecutive sections of 51 data samples, which are cut from the original sensor signals. The time interval is [15 15.25] (second).

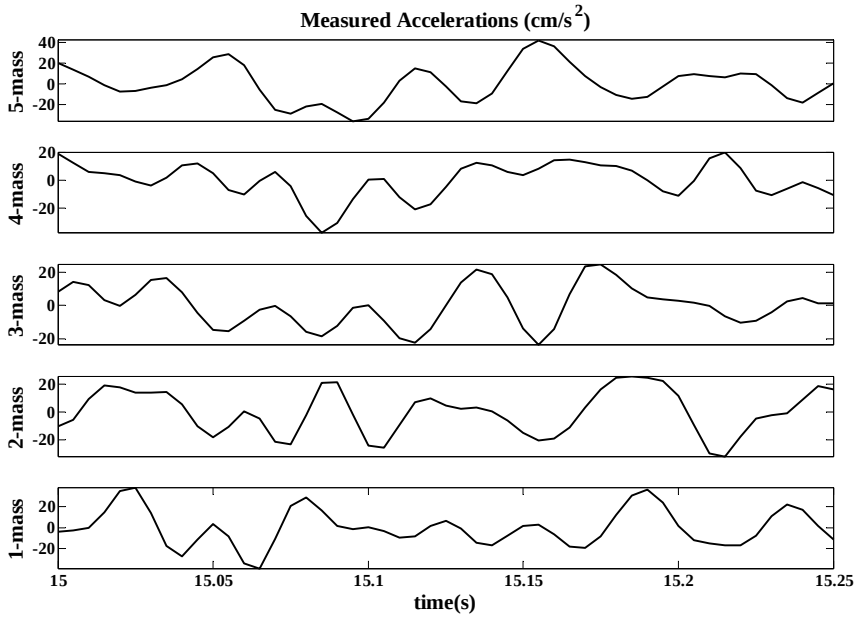

Figure 2.3: Data length of 51: the sections of data samples ([15 15.25] second) cut from the original sensor signals.

For briefty, we only give the analysis results of the acceleration data samples from the fifth mass. The maximal model order is set to be $p_{\max} = 20$. Figure 2.4 plots the 20 AR parameters estimated by using the Burg's method, least squares method and Yule-Walker method respectively. Figure 2.5 shows the estimated prediction error variances for three methods. The prediction error variance in case of the Yule-Walker method is greatly larger than those for the Burg's method and the least squares method. That's to say, the Yule-Walker method does not yield a correct AR model for the data samples with a small data length. The causes of poor Yule-Walker estimates for small data length were discussed in Stoica et al. (1997) and De Hoon et al. (1996). An intuitive explanation for this phenomenon is that the Yule-Walker method uses the biased autocovariance sequence estimates, but not the unbiased autocovariance sequence estimates as the least squares method does (see Section 2.2.2).

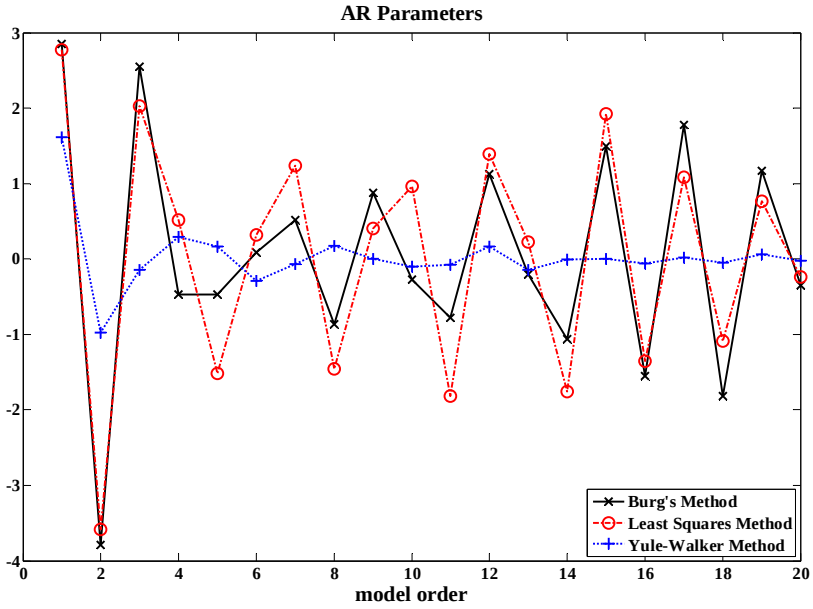

Figure 2.4: Data length of 51: the estimated AR parameters of AR models fitted to the accelerations from the fifth mass, in each case of the Burg's method, the least squares method and the Yule-Walker method.

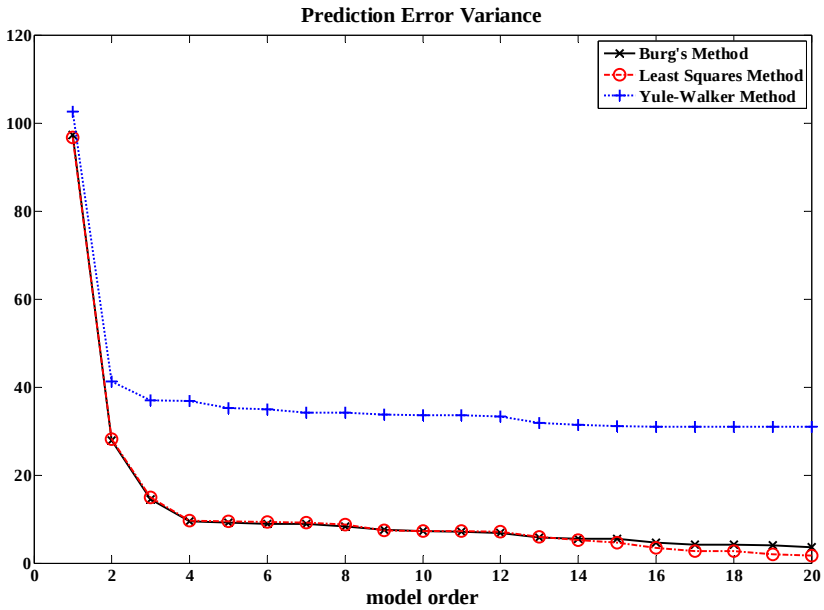

Figure 2.5: Data length of 51: the estimated prediction error variances of AR models fitted to the accelerations from the fifth mass, in each case of the Burg's method, the least squares method and the Yule-Walker method.

Figure 2.6 shows the polar plots of estimated poles for the three methods respectively. It's known that the pole locations indicate the stability of the AR model. As seen in the second panel of Figure 2.6, the least squares method leads to an unstable model, because of the four poles locating outside the unit circle, which are marked by the red circles. The poles of the estimated models by the other two methods are entirely located inside the unit circle, whereby fulfilling the condition for stability.

However, it should be noted that the poles outside the unit circle are related to the high-order AR parameters. Hence the stability of the estimated AR model is possibly guaranteed by selecting the lower model order, if the model order selection is considered, which will be discussed later in this section.

Among three methods, the Yule-walker method can't yield accurate estimates of AR parameters for small data length, and the least squares method sometimes lacks stability of estimated AR model. While the Burg's method is the only reliable AR parameter estimation method, yielding accurate parameter estimates as well as a guaranteed stable AR model.

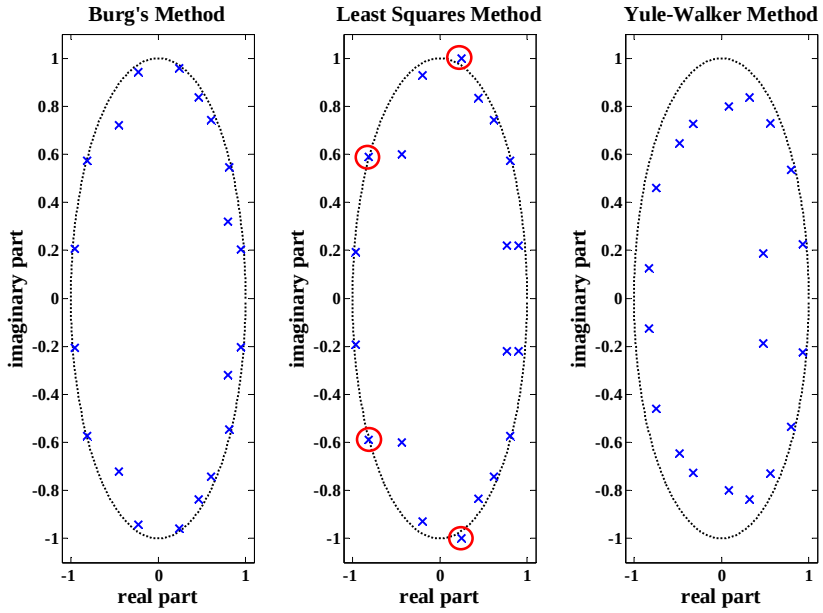

Figure 2.6: Data length of 51: the polar plots of the estimated AR models fitted to the accelerations from the fifth mass, in each case of the Burg's method, the least squares method and the Yule-Walker method.
(The red circle indicates that the pole is located outside the unit circle)

Data length of 201

We here consider a moderately larger data length case. Figure 2.7 shows a consecutive section of 201 data samples, which goes through 1 second interval. The time interval is [17 18] (second).

In the same way, Figure 2.8 and Figure 2.9 give the results of estimated AR parameters and prediction error variances of the first 20 orders, in each case of the Burg's method, the least squares method and the Yule-Walker method. It would be expected that the least squares method and the Burg's method lead to the almost same results of parameter estimates, as shown in Figure 2.9. Compared with the above two, the result of the Yule-Walker method is the worst one. It could be concluded that, even for moderately larger data length, the Yule-Walker method doses not yield good parameter estimates.

The pole locations for three parameter estimation methods are plotted in Figure 2.10. All estimated AR models are guaranteed to be stable in this case.

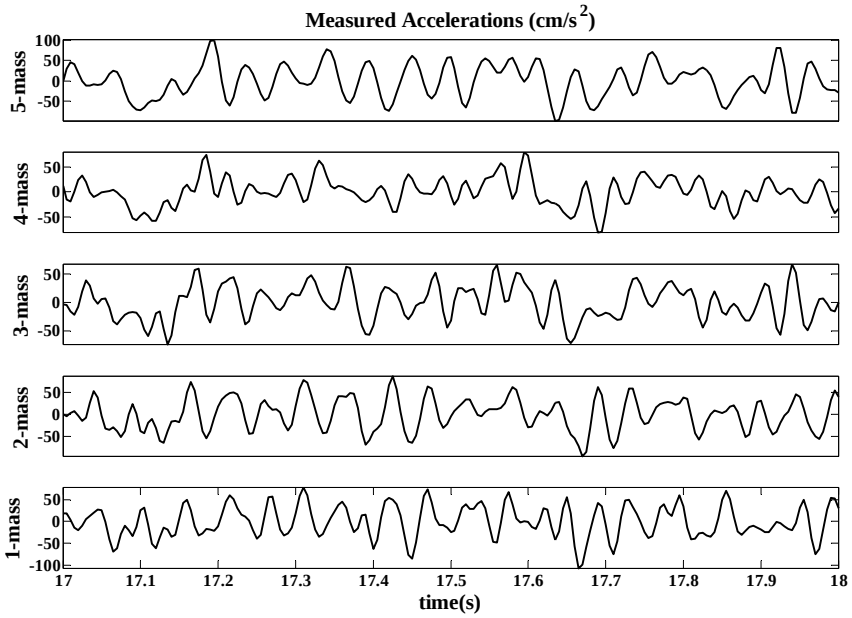

Figure 2.7: Date length of 201: the sections of data samples ([17 18] second) cut from the original sensor signals.

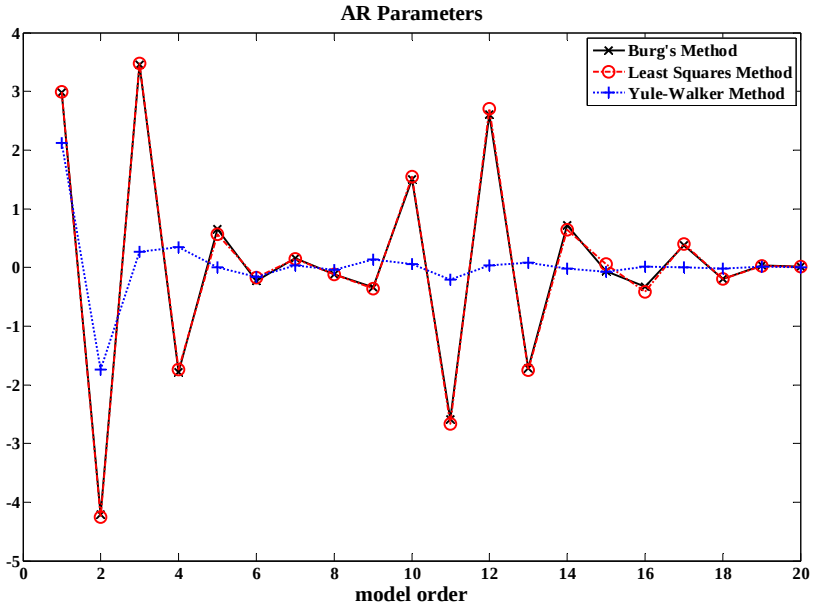

Figure 2.8: Data length of 201: the estimated prediction error variances of AR models fitted to the accelerations from the fifth mass, in each case of the Burg's method, the least squares method and the Yule-Walker method.

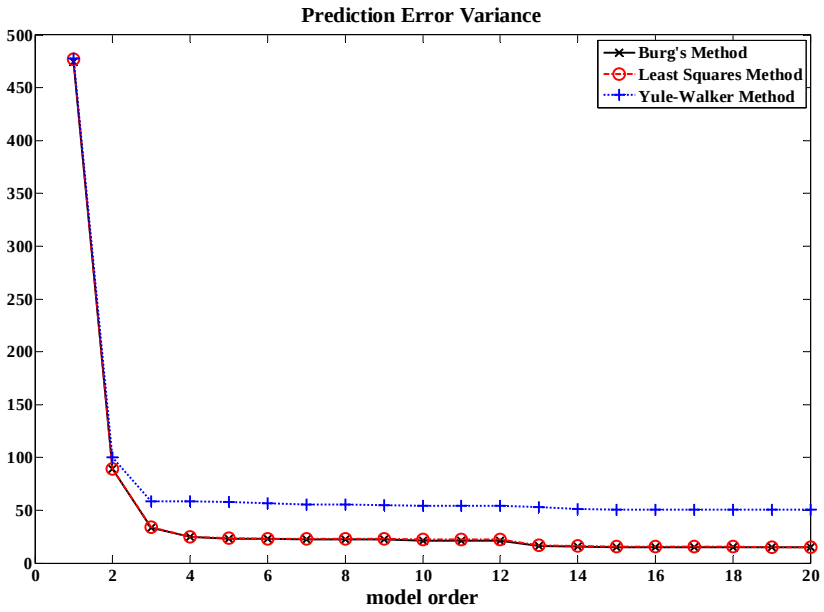

Figure 2.9: Data length of 201: the estimated prediction error variances of AR models fitted to the accelerations from the fifth mass, in each case of the Burg's method, the least squares method and the Yule-Walker method.

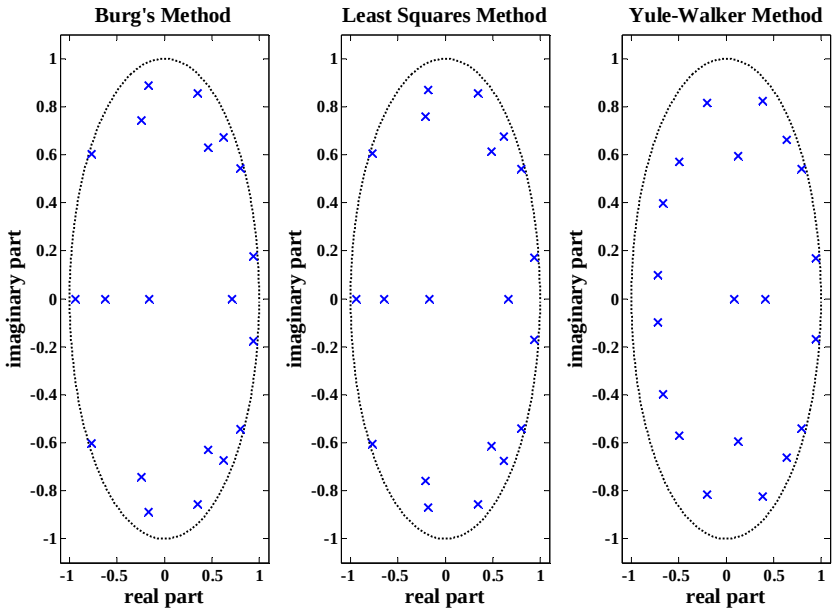

Figure 2.10: Data length of 201: the polar plots of the estimated AR models fitted to the accelerations from the fifth mass, in each case of the Burg's method, the least squares method and the Yule-Walker method.

Data length of 401

In this section, we consider a larger data length case. Figure 2.11 shows a consecutive section of 401 data samples, which goes through 2 second interval. The time interval is [18 20] (second).

Similarly, Figure 2.12 and Figure 2.13 give the results of estimated AR parameters and prediction error variances of the first 20 orders for each method. It is seen from the figures that, the Yule-Walker method may lead to nearly the same parameter estimates as the other two for the large data samples. It can be concluded that each of the three parameter estimation methods performs well when fitting the data samples with large data length.

Figure 2.14 shows the results of pole locations, in each case of the three parameter estimation methods. The estimated AR models all perform well in stability. It is confirmed that the instability led by the least squares method appears infrequently, thereby it's not a serious drawback.

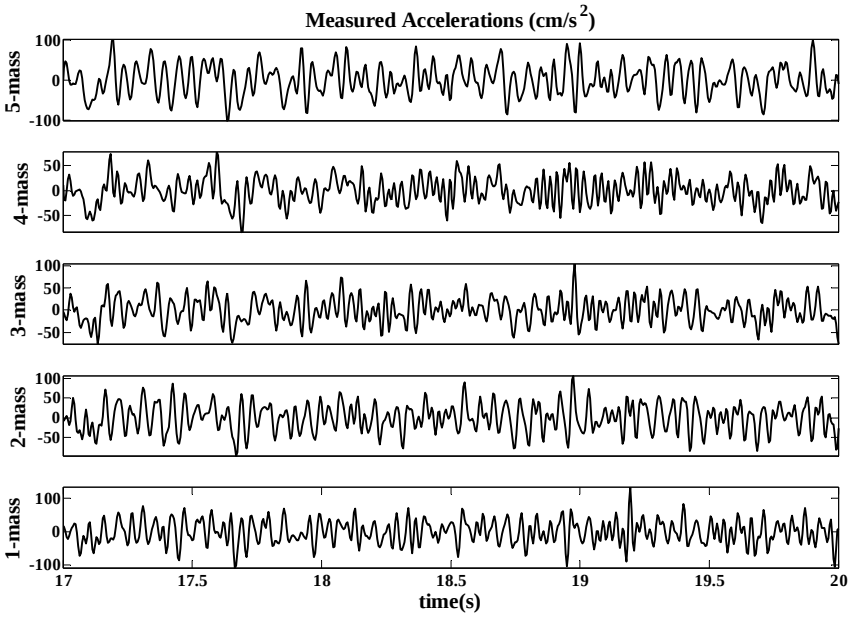

Figure 2.11: Data length of 401: the sections of data samples ([18 20] second) cut from the original sensor signals.

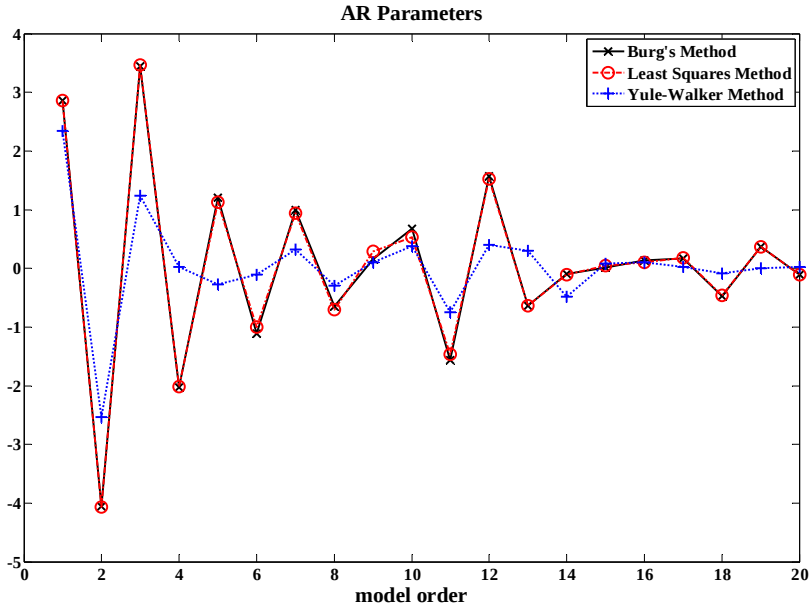

Figure 2.12: Data length of 401: the estimated prediction error variances of AR models fitted to the accelerations from the fifth mass, in each case of the Burg's method, the least squares method and the Yule-Walker method.

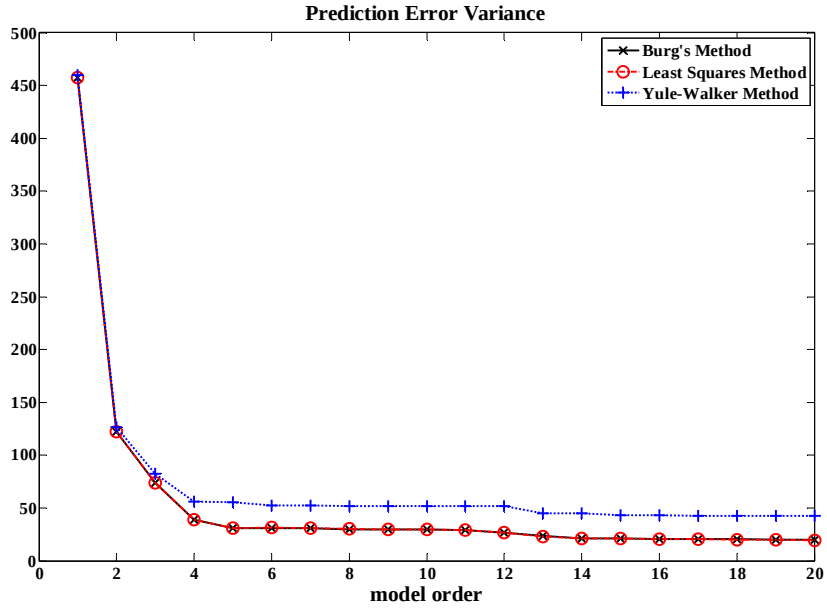

Figure 2.13: Data length of 401: the estimated prediction error variances of AR models fitted to the accelerations from the fifth mass, in each case of the Burg's method, the least squares method and the Yule-Walker method.

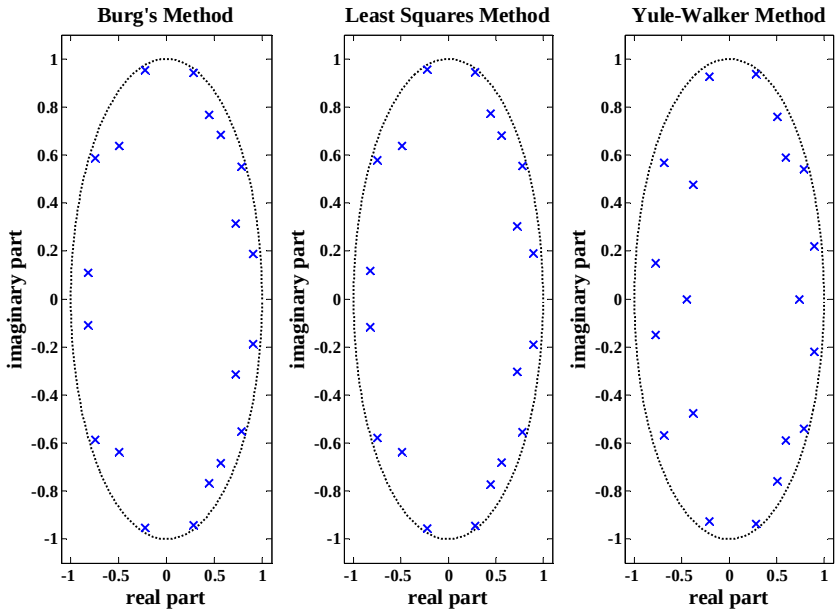

Figure 2.14: Data length of 401: the polar plots of the estimated AR models fitted to the accelerations from the fifth mass, in each case of the Burg's method, the least squares method and the Yule-Walker method.

2.4.2 Order Selection

Secondly, the acceleration signals measured from the shake table test are used to test four model order selection criteria, introduced in Section 2.3:

1. The Final Prediction Error Criterion (FPE);
2. The Akaike Information Criterion (AIC);
3. The Bayesian AIC (BIC);
4. The Schwarz Bayesian Criterion (SBC).

The various acceleration signals from different locations have been evaluated. For briefty, we here only give an example of the analysis performed on the data samples from the fifth mass. The same three data lengths as the above Section 2.6.2 are used, that is data length of 51, 201 and 401. For giving a comparison of different criteria, the prediction error variances are obtained by using the same estimation method, the Burg's method. Then, the optimal model orders, based on the different definitions of the relative prediction error variances, can be obtained by the above four criteria.

We first plot relative prediction error variances against the model order. The graph will, in general, show a definite local minimum value at a particular value at which the criterion attains the appropriate order of the model. From the various relative prediction error variances according to four criteria, the optimal model orders are decided by local minimum values. Figure 2.15, Figure 2.16 and Figure 2.17 show the relative prediction error variances in the cases of three data length, respectively. Table 2.1, Table 2.2 and Table 2.3 give the results of optimal model orders selected by four criteria in the cases of three data length, respectively. .

It can be seen that, there is no apparent divergences of results for the different criteria and different data length in this case. As shown in the Table 2.1, Table 2.2 and Table 2.3, the optimal orders 4 or 5 are frequently selected in different cases. Hence, it is concluded with confidence, the optimal order for the acceleration data samples of this shake table test should be selected as 4 or 5. In fact, we used the different parameter estimation methods and order selection criteria on the data samples from the other masses, and obtained the almost same results.

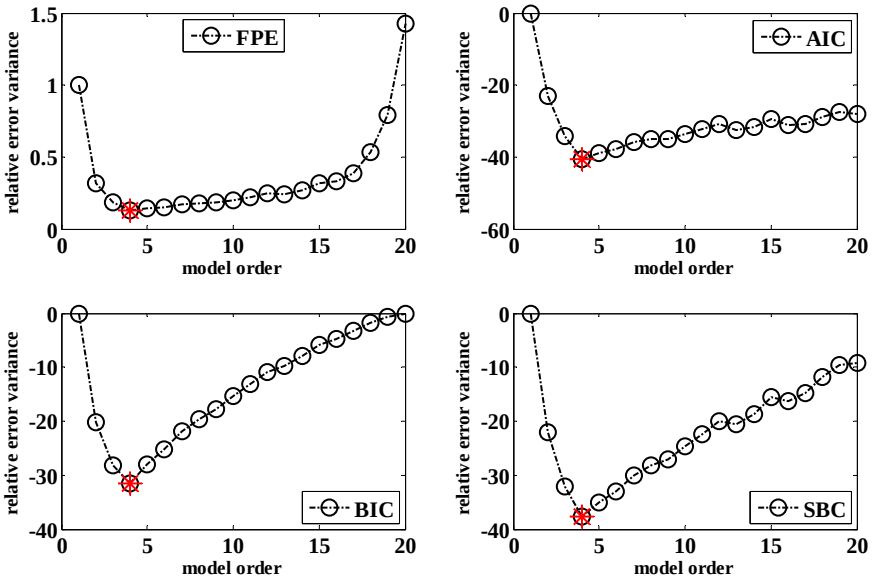

Figure 2.15: Data length of 51: model order selection in each case of the Final Prediction Error Criterion (FPE); the Akaike Information Criterion (AIC); the Bayesian AIC (BIC) and the Schwarz Bayesian Criterion (SBC).

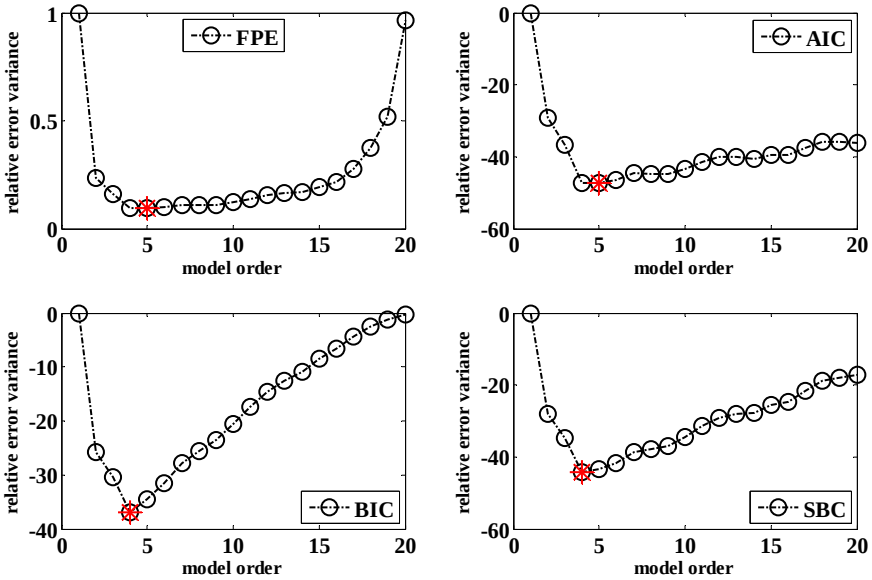

Figure 2.16: Data length of 201: model order selection in each case of the Final Prediction Error Criterion (FPE); the Akaike Information Criterion (AIC); the Bayesian AIC (BIC) and the Schwarz Bayesian Criterion (SBC).

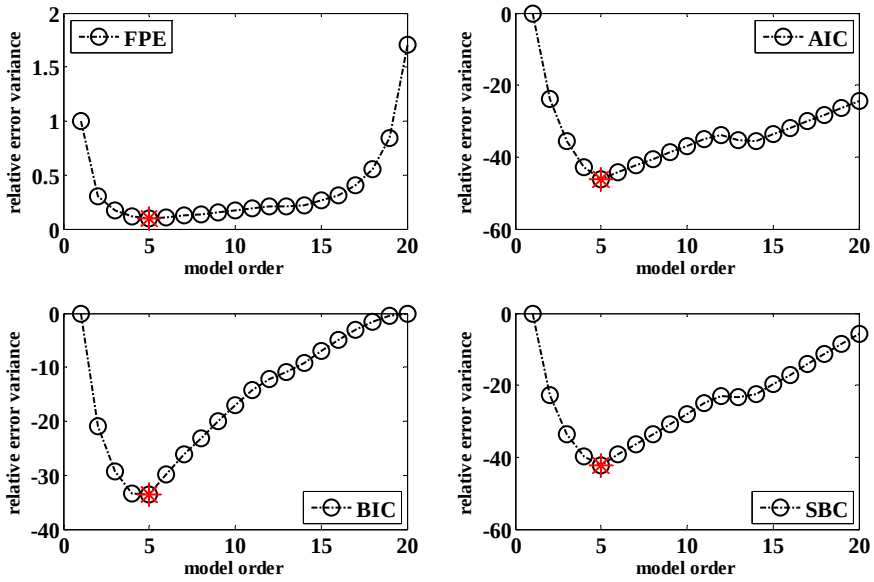

Figure 2.17: Data length of 401: model order selection in each case of the Final Prediction Error Criterion (FPE); the Akaike Information Criterion (AIC); the Bayesian AIC (BIC) and the Schwarz Bayesian Criterion (SBC).

Table 2.1: Optimal orders selected in the case of data length of 51.

Criterion	FPE	AIC	BIC	SBC
Optimal Order	4	4	4	4

Table 2.2: Optimal orders selected in the case of data length of 201.

Criterion	FPE	AIC	BIC	SBC
Optimal Order	5	5	4	4

Table 2.3: Optimal orders selected in the case of l data length of 401.

Criterion	FPE	AIC	BIC	SBC
Optimal Order	5	5	5	5

Summary

In this chapter, we have introduced some widely used model estimation methods for the AR models such as the Yule-walker method, the least squares method and the burg's method. Four model order selection criteria, which are FPE, AIC, BIC and FPE criteria, have also been introduced. To evaluate the various methods and criteria, some illustrated examples were given then.

The estimation methods behaved differently for the different data lengths. In the case of short data length, the Yule-Walker method performed the worst while the Burg' method and the least squares methods yielded nearly the same results. On the other hand, three methods all perform well in the case of large data length. An intuitive explanation for poor Yule-Walker estimates for small data length is that the Yule-Walker method uses the biased autocovariance sequence estimates, but not the unbiased autocovariance sequence estimates as the least squares method does.

On the stability, the Burg's method and the Yule-Walker warranted the estimated AR model to be stable in each case, while the least squares method appeared unstable in AR modeling infrequently. By comparison, the Burg's method is the only reliable AR parameter estimation method in each case of data length, yielding accurate parameter estimates as well as a guaranteed stable AR model.

In addition, four famous model selection criteria, such as FPE, AIC, BIC and SBC have also been evaluated on the data samples with different lengths. Almost the same results were obtained by four criteria in each case. Despite of this, the disagreements on optimal order selection may arise in the other cases. Therefore, the different criteria will also be applied in the following chapters.

Chapter 3

Distance Measure

This chapter discusses two distance measures of AR models: one is the Itakura distance, and the other is the cepstral distance. The distance measures of AR model have been successfully applied in image, speech recognition, and biological, neurological sequences comparison. In this research, we are interested in the novel applications of two distance measures for damage detection and damage localization for structural health monitoring. The distance measures of AR models are considered as the damage indicators.

We first introduce the definitions of the two distance measures. After then, the performances of the damage indicators defined as the distance measures are evaluated by simulation verifications, which are conducted on a five storey building model. The analysis on the acceleration data samples are given, including the order selection and model stability. In the end of this section, various damage scenarios are simulated, in the case of different damage severities and different damage locations. The performances of the damage indicators to identify the different scenarios are tested.

3.1 Two Distance Measures of AR models

Typical applications on time series deal with tasks like prediction, forecasting, system identification. In civil engineering application, the AR model has been a fast and efficient tool to parameterize dynamic responses (Mita, 2003). Estimation of system transfer function from ambient vibration responses is a difficult task in the absence of

excitations. However, the advantages of the AR modelling for ambient vibration over the conventional nonparametric frequency domain methods have been discussed (Pardoen 1983, Kadakal et al. 1996). Thus, the AR model and the multivariate AR model were successfully used to identify structural dynamic characteristics of system subjected to ambient excitations (He et al. 1997, Huang 2001).

On the other hand, the applications of time series deal with tasks like classification, clustering, anomaly detection, noise removal. For SHM, the AR models have been receiving increasing attention that the AR parameters were treated as damage indicators to estimate structural damage. Worden et al. (2000) considered statistical process control approach to damage detection, using the mean and variance of the residuals of the AR model to form the statistical process control charts. A statistical pattern recognition methodology was presented by Sohn et al. (2001). The dynamic signals recorded were modeled using autoregressive (AR) time series models. By statistically examining changes in AR coefficients, they could classify signals from either undamaged or damaged systems. Mattson et al. (2006) chose the standard deviation of the residual of vector AR (VAR) model as the damage indicator. De Lautour et al. (2006) used the AR coefficients as input features into an Artificial Neural Network (ANN). The damage and its extent were identified by observing the changes in AR coefficients. However, a disadvantage of these methods is that, without pattern recognition tools, they are unable to damage localization or quantification.

The application of time series on damage detection relies heavily on the ability to measure the similarity and dissimilarity between time series (Agrawal et al. 1993 and 1995, Jagadishi 1995, Kalpakis 2001). Therefore, in this research, we offer a new strategy of time-series analysis to understand the dynamic responses recorded on a civil infrastructure, by taking into account the variability of distance measure as a result of structural damage. The distance between the two AR models is considered to be correlated with the position and severity of the damage. Hence, the distance measures between AR models are defined as the damage indicators. Two distance measure methods are introduced in the next sections: one is the Itakura distance (Itakura 1975, Rabiner et al. 1993); the other is the cepstral distance (Martin 2000,). Next, we give the definitions of the distance measures.

3.1.1 Cepstral Distance

The first distance measure we are interested in is a weighted Euclidean cepstral distance, which is proposed by Martin (2000).

The cepstrum of a stochastic process is defined as the "inverse Fourier transform of the logarithmic power spectrum". The cepstrum was firstly introduced by Bogert et al. (1963), who used it for the detection of echoes. Cepstrum has been applied in a variety of areas including audio processing, speech processing, geophysics, machine diagnostics, and others (Oppenheim et al. 2004, Ulrych 1971, Stockham 1972, Davis et al. 1980, and Wismer's application note).

Furthermore, the cepstrum has been also used for measuring the distance between two signals. Tohkura (1987) tested a weighted cepstral distance on a speaker-independent isolated word recognition system. The experimental results show that the weighted cepstral distance measure works substantially better than both the Euclidean cepstral distance and the log likelihood ratio distance measures across two different databases. Basseville et al. (1989) presented some general tools for measuring distances between two parametric models, either the spectral distance measures or the parametric spectral distance measures. Kalpakis et al. (2001) used the unweighted cepstral distance to cluster time series, and found that it performs much better than other widely used methods such as discrete Fourier transform and principal component analysis and so on. De Cork et al. (2000, 2002a, 2002b, 2003 and 2004) related the weighted cepstral distance proposed by Martin (2000) to the subspace angles, and gave a graphical interpretation of the cepstral distance, which is related to the area enclosed by the polar plot of the logarithm of the ratio of the transfer functions of two models. Bissacco (2001) applied the subspace angles, proposed by De Cork et al., to recognize human gaits. Boets et al. (2005 and 2006) considered using the Martin's weighted cepstral distance for time series clustering. The best results were obtained with the weighted cepstral distance compared with the other distance measures including the unweighted cepstral distance, the distance between spectra, the $\mathbf{H}_2$ distance and the $\mathbf{H}_\infty$ distance.

In this research, we concern about the Martin's weighted cepstral distance, which is supposed to measure the distance between two parametric models. Martin listed the drawbacks of distance measure in the form of weighted Euclidean distance of AR parameters, such as the difficulty of finding good weights, the lack of system

theoretic properties and the lack of mathematical properties. After then, the cepstral distance measure was proposed (Martin 2000).

Next, we introduce this cepstral distance measure. The cepstral distance between AR models can be derived from a cepstral distance between autoregressive moving-average (ARMA) models.

An ARMA process is given by

$$x(n) = -\sum_{i=1}^{p} a(i)x(n-i) + \sum_{j=0}^{q} b(j)e(n-i), \qquad (3.1.1)$$

where $a(i)$ and $b(j)$ are the AR and MA coefficients, respectively. p and q are the optimal model orders of the AR and MA processes, respectively, and $e(n)$ is a white noise process with zero mean and variance σ^2.

The transfer function of a stable, minimum ARMA process has the form in the z domain

$$H(z) = \frac{\sum_{j=0}^{q} b(j)z^{-j}}{\sum_{i=0}^{p} a(i)z^{-i}} = \frac{\prod_{j=1}^{q}\left(1-\beta(j)z^{-1}\right)}{\prod_{i=1}^{p}\left(1-\alpha(i)z^{-1}\right)} \qquad (3.1.2)$$

where $\alpha(i)$ and $\beta(j)$ are the poles and zeros of the ARMA model.

The power cepstrum is the inverse Fourier transform of the logarithm of its power spectrum $P(z)$ (Oppenheim et al. 1975):

$$\log P(z) = \log\left\{\sigma^2 H(z)\overline{H}\left(z^{-1}\right)\right\} = \sum_{n\in z} C(n)z^{-n} \qquad (3.1.3)$$

where $C(n)$ are the cepstrum coefficients.

Substituting (3.1.2) into (3.1.3), the logarithm of the power spectrum becomes

$$\log P(z) = -\sum_{i=1}^{p} \log\left|z-\alpha(i)\right|^2 + \sum_{j=1}^{q} \log\left|z-\beta(j)\right|^2 + \log\sigma^2, \qquad (3.1.4)$$

Then, the power cepstrum of the ARMA model can be expressed in terms of the poles and zeroes as

$$c[n]=\begin{cases}\dfrac{1}{n}\left[\sum_{i=1}^{p}\alpha^{n}(i)-\sum_{j=1}^{q}\beta^{n}(j)\right], & n>0,\\ \log\sigma^{2}, & n=0,\\ \dfrac{1}{n}\left[\sum_{i=1}^{p}\overline{\alpha}^{-n}(i)-\sum_{j=1}^{q}\overline{\beta}^{-n}(j)\right], & n<0,\end{cases} \qquad (3.1.5)$$

Since the poles and zeroes occur in complex conjugate pairs, then the above expression becomes

$$c(n)=\begin{cases}\dfrac{1}{|n|}\left[\sum_{i=1}^{p}\alpha^{|n|}(i)-\sum_{j=1}^{q}\beta^{|n|}(j)\right], & n\neq 0,\\ \log\sigma^{2}, & n=0,\end{cases} \qquad (3.1.6)$$

For two ARMA models M' and M'' with the associated cepstrum coefficients $c'(n)$ and $c''(n)$, the cepstral distance between the models could be defined by a weighted Euclidean distance between cepstrums:

$$d(M',M'')^{2}=\sum_{n=1}^{\infty}n\left|c'(n)-c''(n)\right|^{2} \qquad (3.1.7)$$

Since the cepstral metric is a Euclidean distance, the following property on the set of ARMA models holds

$$d(M'M''',M''M''')=d(M',M'') \qquad (3.1.8)$$

In other words, if two models M' and M'' are passed through the same linear filter with model M''', their mutual distance is unaltered.

Therefore, suppose that $H'_{ARMA}(z)=\dfrac{b'(z)}{a'(z)}$ and $H''_{ARMA}(z)=\dfrac{b''(z)}{a''(z)}$ are the transfer functions of two ARMA models M' and M'', and that the third ARMA model M''' has transfer function $H'''(z)=\dfrac{1}{b'(z)b''(z)}$.

Then two AR models N' and N'' with transfer functions can be constructed as followings:

$$\begin{cases} H'_{AR}(z) = H'_{ARMA}(z)H'''(z) = \dfrac{1}{a'(z)b''(z)} \\ H''_{AR}(z) = H''_{ARMA}(z)H'''(z) = \dfrac{1}{a''(z)b'(z)} \end{cases} \qquad (3.1.9)$$

According to the property (3.1.8), there is

$$d(M',M'') = d(N',N''), \qquad (3.1.10)$$

Hence, to measure the distance between ARMA models M' and M'', it is sufficient to consider AR models N' and N'' only.

Furthermore, from the viewpoint of modern spectral analysis, the AR model is proven appropriate to approximate the power spectra with sharp peaks and the spectral peaks can be represented by the poles of AR model. That's to say, the AR poles can indicate strong structural resonances in the system.

Therefore, to distinguish between two segments of vibration responses from structures in different states, the cepstral distance between AR models can be used. Suppose that the structure systems in baseline and unknown states are described by AR models N' and N'' with model orders p', p'' and the associated poles $\alpha'(i), \alpha''(j)$. The cepstral distance measure is defined by

$$d(N',N'') = \log \frac{\prod_{i=1}^{p'}\prod_{j=1}^{p''}(1-\alpha'(i)\overline{\alpha}''(j))\prod_{i=1}^{p''}\prod_{j=1}^{p'}(1-\alpha''(i)\overline{\alpha}'(j))}{\prod_{i=1}^{p'}\prod_{j=1}^{p'}(1-\alpha'(i)\overline{\alpha}'(j))\prod_{i=1}^{p''}\prod_{j=1}^{p''}(1-\alpha''(i)\overline{\alpha}''(j))} \qquad (3.1.11)$$

3.1.2 Itakura Distance

The Itakura distance was initially developed to measure the similarities between voice segments, which are modeled by AR models (Itakura 1975, Gray et al. 1976, Rabiner et al. 1993). Since then, it has been widely applied in neurological signals, biological sequence comparison and others. For examples: Kong et al. (1995, 1998, 1999) and Estrada et al. (2004, 2005) tested the effectiveness of the Itakura distance measure when applied to the electroencephalogram (EEG) signals. Muthuswamy et al. (1998) presented the measuring of the Itakura distance to quantify the differences between the spectra of two neurological signals and found the AR model improves the resolution of the spectra. Pham (2006a, 2006b, 2007) considered using both cepstral distance and Itkura distance for finding the similarities between related sequences of DNA or protein.

The dynamic responses from structures can be in a sense seemed as the sound of structures. Therefore, we are interested in the novel application of Itakura distance measure for damage detection in civil engineering field. Suppose that the AR model of a segment of vibration response from structure (say acceleration output) in baseline state can be expressed by:

$$x(n)+\sum_{i=1}^{p} a_x(i)x(n-i)=e_x(n) \qquad (3.1.12)$$

Then, the AR model of a segment in unknown state is given by:

$$y(n)+\sum_{i=1}^{p} a_y(i)y(n-i)=e_y(n) \qquad (3.1.13)$$

where $a_x(i)$ and $a_y(i)$ are the parameters describing the vibration system and white noise $e_x(n)$ and $e_y(n)$ are the unpredictable parts in the vibration signals $x(n)$ and $y(n)$. Suppose that the optimal model order for both time series is p. The AR parameters of two time series can be written in compact from:

$$A_x=\begin{bmatrix}1 & -a_x(1) & -a_x(2) & \cdots & -a_x(p)\end{bmatrix}^T \qquad (3.1.14)$$

$$A_{\mathbf{y}}=\begin{bmatrix}1 & -a_y(1) & -a_y(2) & \cdots & -a_y(p)\end{bmatrix}^T \qquad (3.1.15)$$

The AR parameters $a_x(i)$ can be optimally determined by minimizing the minimum mean square error (MSE),

$$\min_{a_x(i)} E\left\{\left(x(n)-\sum_{i=1}^{p} a_x(i)x(n-i)\right)^2\right\} \qquad (3.1.16)$$

The MSE can also be expressed as

$$\xi_{11} = A_x{}^T R_x A_x \qquad (3.1.17)$$

where R_x is the covariance matrix of signal $x(i)$

$$R_x = \begin{bmatrix} r_x(0) & r_x(1) & \cdots & r_x(p) \\ r_x(1) & r_x(0) & \cdots & r_x(p-1) \\ \vdots & \vdots & \ddots & \vdots \\ r_x(p) & r_x(p-1) & \cdots & r_x(0) \end{bmatrix} \qquad (3.1.18)$$

The individual element in the matrix $r_x(k)$ is the covariance function of signal $x(i)$, which is given by

$$r_x(m) = \frac{1}{N}\sum_{n=1}^{N-m} x(n)x(n+m), \qquad m = 0,1,2,\cdots,p \qquad (3.1.19)$$

Actually (3.1.18) and (3.1.19) are equivalent to the covariance matrix in (2.2.12) and the standard biased autocovariance sequence in (2.2.17).

Suppose that the signals $x(n)$ pass through the AR model parameterized by A_y, the MSE will be:

$$\xi_{12} = A_y^T R_x A_y \qquad (3.1.20)$$

Since $a(i)$ are the optimal values from the MSE ξ_{11}, we must have $\xi_{11} \le \xi_{12}$. Only if the signals $x(n)$ and $y(n)$ are from the same system, i.e., two signals have the identical system characteristics, we have $\xi_{11} = \xi_{12}$. When the unknown state is different from the baseline state, the MSE ξ_2 will be larger than ξ_1. Thus, the Itakura

distance, which tests how far the unknown state parameterized by A_y is from the baseline state parameterized by A_x, is defined as

$$d'(A_x, A_y) = \log \frac{\xi_{12}}{\xi_{11}} = \log \frac{A_y{}^T R_x A_y}{A_x{}^T R_x A_x} \qquad (3.1.21)$$

Similarly, the AR parameters $a_y(i)$ can be optimally determined by minimizing the minimum mean square error (MSE),

$$\min_{a_y(i)} E\left\{ \left(y(n) - \sum_{i=1}^{p} a_y(i) y(n-i) \right)^2 \right\} \qquad (3.1.22)$$

The MSE can also be expressed as

$$\xi_{22} = A_x{}^T R_x A_x \qquad (3.1.23)$$

and suppose that the signals $y(n)$ pass through the AR model parameterized by A_x, the MSE will be:

$$\xi_{21} = A_x{}^T R_y A_x \qquad (3.1.24)$$

Similarly, by testing how well the signals $y(n)$ pass through AR model $a(i)$, another Itakura distance measure is given by

$$d''(A_x, A_y) = \log \frac{\xi_{21}}{\xi_{22}} = \log \frac{A_x{}^T R_y A_x}{A_y{}^T R_y A_y} \qquad (3.1.25)$$

where R_y is the covariance matrix of signal $y(i)$:

$$R_y = \begin{bmatrix} r_y(0) & r_y(1) & \cdots & r_y(p) \\ r_y(1) & r_y(0) & \cdots & r_y(p-1) \\ \vdots & \vdots & \ddots & \vdots \\ r_y(p) & r_y(p-1) & \cdots & r_y(0) \end{bmatrix} \qquad (3.1.26)$$

and $r_y(k)$ is the covariance function of signal $y(i)$, which is given by

$$r_y(m) = \frac{1}{N}\sum_{n=1}^{N-m} y(n)y(n+m), \qquad m = 0,1,2,\cdots, p \qquad (3.1.27)$$

Combining two Itakura distance measures (3.1.21) and (3.1.25), a symmetric distance measure can then be obtained:

$$d(A_x, A_y) = \frac{1}{2}\left(d'(A_x, A_y) + d''(A_x, A_y)\right) \qquad (3.1.28)$$

3.2 Numerical Verification

3.2.1 Building Model

To verify the performance of two distance measures for damage detection, simulation studies has been conducted on a five storey shear building model. This model can be simplified as a five degree-of-freedom structure system, as depicted in Figure 3.1. The structure system is subjected to ambient excitations on every mass.

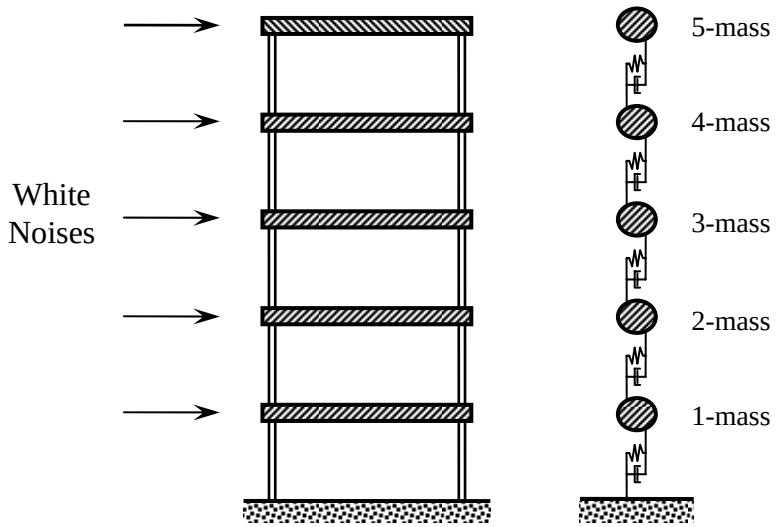

Figure 3.1: Five storey building and its simplified system.

Suppose that the mass of every storey is 100 kg, and the lateral stiffness is 1MN/m. The damping ratio is assumed to be 3% for all modes. The undamaged natural frequencies of the simulated structure system were obtained, as shown in Table 3.1.

Table 3.1: Natural frequencies of simulated building model.

Mode	Natural Frequency (Hz)
1	4.53
2	13.22
3	20.84
4	26.78
5	30.54

The building structure is assumed to be subjected to ambient excitations, which are simulated by multiple white noise processes, each with mean of zero N and variance of 1 N^2. The white noise excitations are assumed to approximate wind or other ambient excitations. We applied the modal superposition algorithm simulate the dynamical responses of the structure system. The acceleration responses for five masses are obtained, as shown in Figure 3.2. In the simulation, the length of data samples is 4001, and the sampling frequency is 200 Hz.

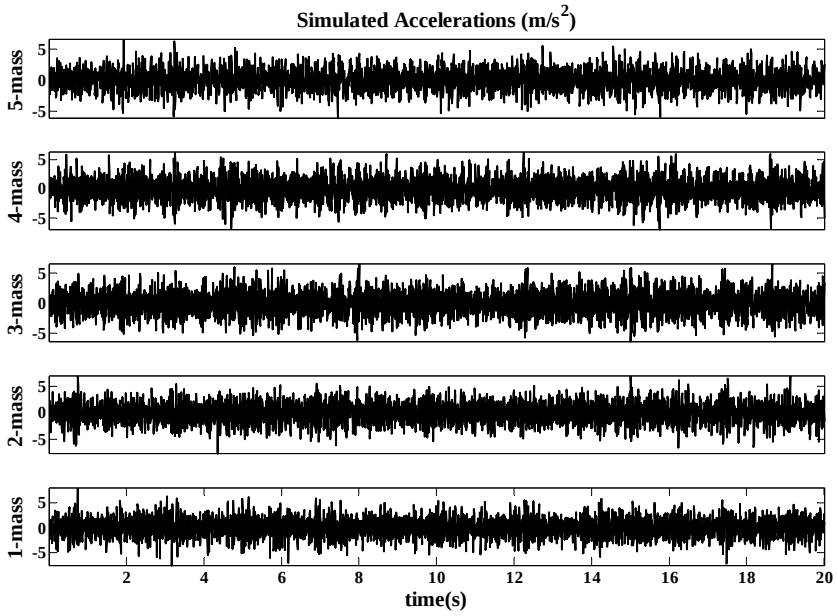

Figure 3.2: Simulated acceleration time histories from each storey of the building model when subjected to ambient forces

3.2.2 Evaluation Method of Distance Measure

In the evaluation, the damage indicator is defined as the distance measure, either the Itakura distance or the cepstral distance. Assume the evaluation of the damage indicator is performed when the damage scenario is unknown. The structure without damage is considered as the baseline state, while the structure with the damage simulated by inter-storey stiffness reduction is considered as the unknown state. The procedure of damage detection using the distance measure is depicted in Figure 3.3:

- Firstly, the vibration signals from building structure, acceleration time histories, are parameterized by AR models.
- Secondly, by using distance measures, either Itakura distance or cepstral distance, the distance between the AR models fitting the acceleration time histories from structure in baseline state and unknown state are measured.
- Finally, decision can be drawn that a large distance indicators a possible damage in the structure.

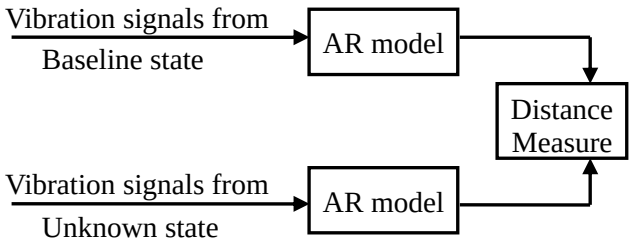

Figure 3.3: Procedure of damage detection by distance measure

3.2.3 Mutually Uncorrelated Ambient Excitations Case

In this case, we consider the mutually uncorrelated ambient excitations. The excitations acting on five masses are simulated by five white noise processes, which are mutually independent and uncorrelated. To observe the correlations among the multiple inputs, we first give the covariance analysis of the excitations by calculating the covariance matrix.

Covariance analysis

Since the ambient excitations are created randomly, the excitations are different for each time, as well as the corresponding covariance matrix. We can't give the theoretical expressions of covariance matrix but can only give the simulation results. For example, we here give a simulation result of the covariance matrices of the multiple inputs and outputs of the structural system.

In this case, the structural responses, the acceleration time histories, were simulated from the structure model in the baseline state. The covariance matrices of the input forces and output accelerations, which act on and response from the undamaged structure, are obtained as follows:

$$R_{in} = 10^4 \times \begin{bmatrix} 1.0015 & 0.0131 & -0.0140 & 0.0246 & -0.0047 \\ 0.0131 & 0.9868 & -0.0080 & -0.0211 & -0.0034 \\ -0.0140 & -0.0080 & 1.0042 & -0.0275 & -0.0067 \\ 0.0246 & -0.0211 & -0.0275 & 0.9987 & -0.0161 \\ -0.0047 & -0.0034 & -0.0067 & -0.0161 & 0.9980 \end{bmatrix}$$

and

$$R_{out} = 3.7597 \times \begin{bmatrix} 1.0402 & -0.2066 & 0.0241 & -0.0059 & -0.0501 \\ -0.2066 & 1.1037 & -0.2268 & -0.0570 & -0.0459 \\ 0.0241 & -0.2268 & 1.0439 & -0.2954 & -0.0450 \\ -0.0059 & -0.0570 & -0.2954 & 1.0237 & -0.2846 \\ -0.0501 & -0.0459 & -0.0450 & -0.2846 & 0.7885 \end{bmatrix}$$

It is well known that, for the linear multiple input multiple output (MIMO) system, the multiple outputs are mutually uncorrelated if and only if the multiple inputs are mutually uncorrelated (Haugh 1976, Hong 1996).

Hence, it can be seen that the covariance matrix of the inputs R_{in} is almost a diagonal matrix, and that of the outputs R_{out} is near to be diagonal. Note that the covariance matrix of outputs is a band matrix, which is similar to the shape of the stiffness matrix of the structure system.

Model analysis

Similar to the analysis in Section 2.4.1, we use the three model parameter estimation methods, Burg's method, Least Squares Method and Yule-Walker Method, to parameterize the simulated acceleration time histories.

For example, we give the results of an acceleration time histories, which is from the first storey of the building structure in the baseline state. For comparing the different model orders, the models with a maximal order of 100 are estimated.

Figure 3.4 shows the prediction error variances of three methods with a maximal model order of 100. It is seen that the three methods yield almost identical results when the model orders less than 40, and after then the Burg's method and the least squares perform a litter better than the Yule-Walker method. The three methods are all qualified for the task since the model order of 40 is generally enough.

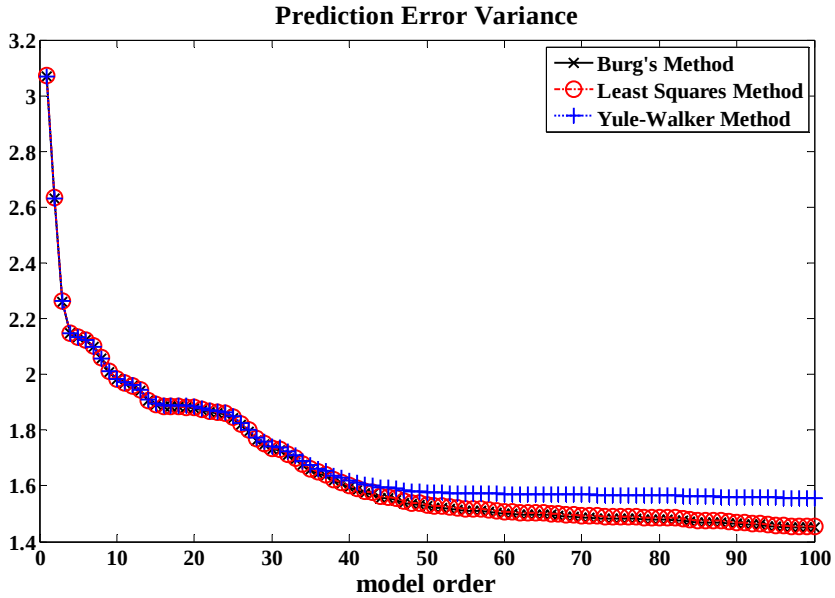

Figure 3.4: Estimated prediction error variances of three model parameter estimation methods with the maximal order of 100, in the case of mutually uncorrelated ambient inputs and the baseline state of building structure.

Next, the model order selection is analyzed by four criteria: the Final Prediction Error Criterion (FPE); the Akaike Information Criterion (AIC); the Bayesian AIC (BIC) and the Schwarz Bayesian Criterion (SBC). Here, the prediction error variances were calculated by using the Burg's method. For comparing the different model orders, the

models with a maximal order of 50 are estimated.

Figure 3.5 plots an example of the results of optimal order selection by four criteria. Decided by the local minimum, four criteria give the same results of optimal model order of 3, as shown in Table 3.2.

For the various acceleration signals from different masses, the corresponding AR models have been evaluated for model order selection. Also the various damage scenarios should be considered. The similar results of optimal orders were obtained for different cases. The FPE, AIC, SBC and SBC criteria give the same optimal order equal to or near to 3. Therefore, the order of 3 is selected to estimate the AR models and to measure the distance between AR models.

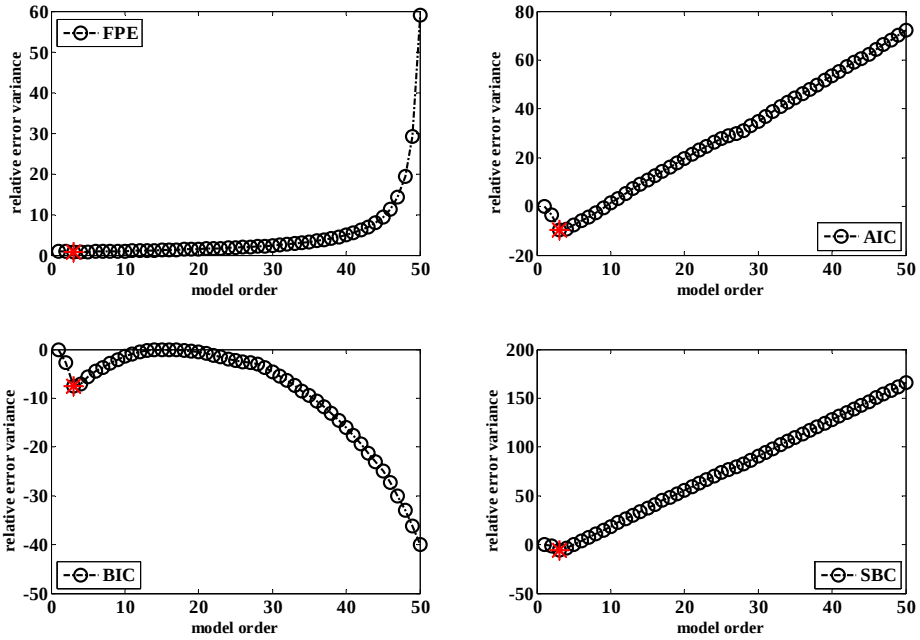

Figure 3.5: Optimal model order selected by the FPE, AIC, BIC and SBC criteria, with the maximal order of 50, in the case of mutually uncorrelated ambient inputs and the baseline state of building structure.

Table 3.2: Optimal orders selected in the case of mutually uncorrelated ambient excitations

Criterion	FPE	AIC	BIC	SBC
Optimal Order	3	3	3	3

Distance measures

To simulate the structural damage, the inter-storey stiffness reduction ratio, which is the most typical damage scenario, is assumed to occur on the structural model. Single damage cases occur on each storey respectively, which are '1 storey damage', '2 storey damage'…, and '5 storey damage'. The inter-storey stiffness reduction between the first mass and the base is called as '1-storey damage', and The inter-storey stiffness reduction between the first and second masses is called as '2 -storey damage', and the rest may be deduced by analogy.

For evaluating the sensitivity of the proposed damage indicator, minor damage severities are selected, which are 2% , 4% , 6% , 8% and 10% stiffness reduction. Hence, there are a total of 25 damage scenarios.

The measurement noises are assumed to be white noise processes, which are added to the acceleration time histories. The every acceleration response has been added by the measurement noise of 10% noise level, which is the ratio of root mean square (RMS) of sensor noises to acceleration responses. The corresponding signal over noise ratio (SNR) is $SNR = 20dB$.

Following the procedure of damage detection by distance measures, depicted in Figure 3.3, the distance measures between AR models are defined as the damage indicators for damage detection. Two distance measures introduced in Section 3.1.1 and Section 3.1.2, the Itakura distance and the cepstral distance, were both evaluated. Firstly, the Burg's method was used to estimate the AR parameters. The optimal model order of 3 obtained above was selected as the model order not only for model parameter estimation but also for distance measures. Therefore, the first 3 AR parameters estimated by the Burg's method were used to obtain the distance measures. For all the damage scenarios, 25 corresponding damage indicators were obtained, either by (3.1.11) or (3.1.28).

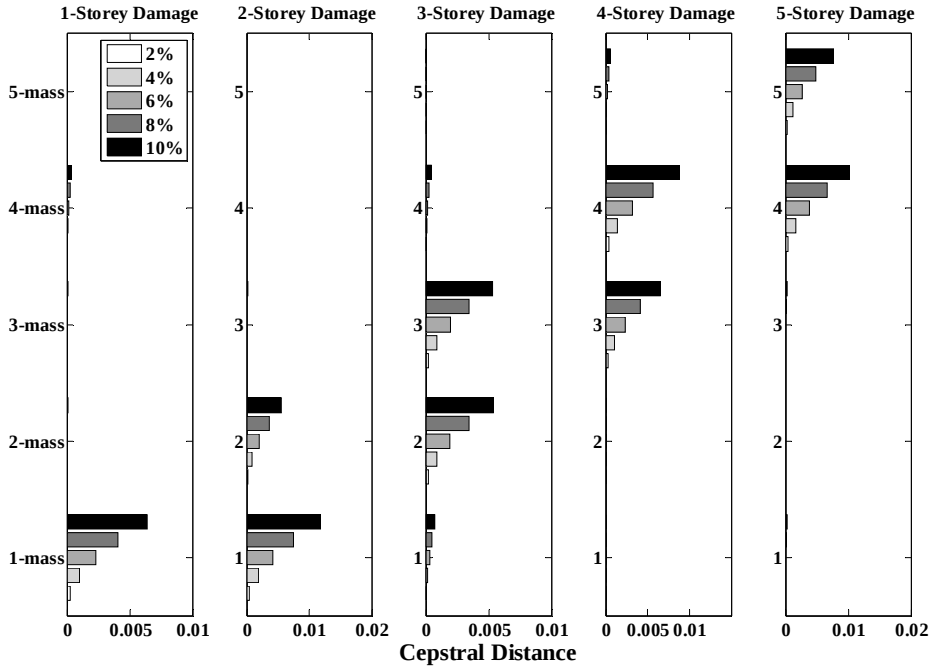

Figure 3.6: Cepstral distances in the case of mutually uncorrelated ambient excitations.

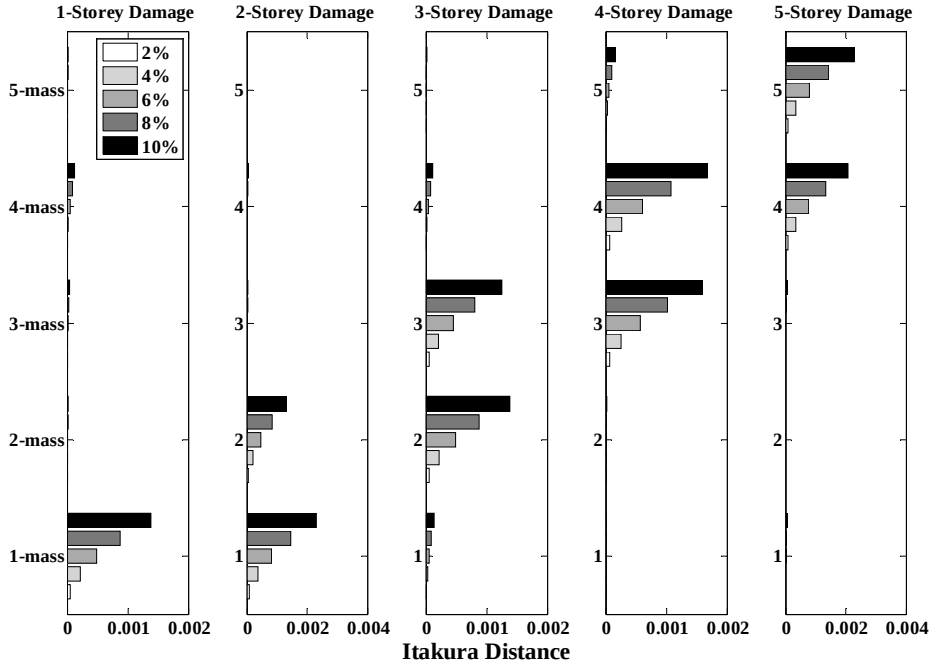

Figure 3.7: Itakura distances in the case of mutually uncorrelated ambient excitations.

Figure 3.6 shows the results of cepstral distance measures, and Figure 3.7 shows those of Itakura distance. Results show that both two methods are capable of identifying the damage and its locations. Since the damage occurs between two adjacent storeys, the distance measures for these two storeys are a lot larger than the others. As shown in both figures, the magnitude differences of damage indicators can exactly imply the possible damage location.

It should be noted that the gray level in the bar graph implies damage level. The distance measures increase monotonically with the inter-storey stiffness reduction, which provides the potential to estimate the damage severity. However, for real damage quantification, the exact relation between the damage indicator and damage severity should be further evaluated carefully.

Actually, the optimal orders near to 3, such as 2 or 4, have been obtained infrequently in some cases. The corresponding AR parameters and distance measure were also calculated. It is found that the similar results of distance measures to Figure 3.6 and Figure 3.7 could be obtained.

3.2.4 Mutually Correlated Ambient Excitations Case

Next, we consider the mutually correlated inputs. The inputs are still five white noise processes acting on every mass, as depicted in Figure 3.1. In this case, we generate five mutually correlated inputs by assuming the white noise processes to be identical.

Different from the above case, there should be strong correlations among the simulated ambient excitations. Therefore, the covariance matrix of the multiple inputs should not be a diagonal matrix. Since that the outputs are mutually uncorrelated only if the inputs are mutually uncorrelated, the outputs are also mutually correlated.

Covariance analysis

In the same way, we here give a simulation example of the covariance matrices of multiple inputs and outputs of the structural system. This example used the acceleration signals from the baseline state, i.e. the undamaged structural model. The covariance matrices of the input forces and output accelerations are obtained by

simulation as follows:

$$R_{in} = 10^4 \times \begin{bmatrix} 0.0407 & 0.0407 & 0.0407 & 0.0407 & 0.0407 \\ 0.0407 & 0.0407 & 0.0407 & 0.0407 & 0.0407 \\ 0.0407 & 0.0407 & 0.0407 & 0.0407 & 0.0407 \\ 0.0407 & 0.0407 & 0.0407 & 0.0407 & 0.0407 \\ 0.0407 & 0.0407 & 0.0407 & 0.0407 & 0.0407 \end{bmatrix}$$

and

$$R_{out} = \begin{bmatrix} 1.6183 & 1.5043 & 1.3370 & 1.2921 & 1.2504 \\ 1.5043 & 1.8681 & 1.7529 & 1.5509 & 1.4882 \\ 1.3370 & 1.7529 & 2.0363 & 1.9457 & 1.7687 \\ 1.2921 & 1.5509 & 1.9457 & 2.2414 & 2.2205 \\ 1.2504 & 1.4882 & 1.7687 & 2.2205 & 2.6677 \end{bmatrix}$$

From the results, it can be seen that the covariance matrices of both inputs and outputs are full matrices. That's to say, there exist strong correlations among the inputs and outputs.

Model analysis

In the same way, three model parameter estimation methods, the Yule-Walker Method, the Least Squares Method, and the Burg's method were used to parameterize the simulated acceleration time histories. For example, we also give the results of the baseline state of the building structure. The setting factors for simulation are the same as the above case: the length of data samples is selected as 4001, the sampling frequency is 200 Hz, and the models with a maximal order of 100 are estimated.

Figure 3.8 shows the prediction error variances of three methods with a maximal model order of 100. The results are similar to the results of mutually uncorrelated excitations case, as shown in Figure 3.4. The three methods yield almost identical results when the model orders less than 60, while the divergence starts to appear only if the model order is larger than 60. It can be concluded that, in general, the three methods are all qualified for the large data sample length case.

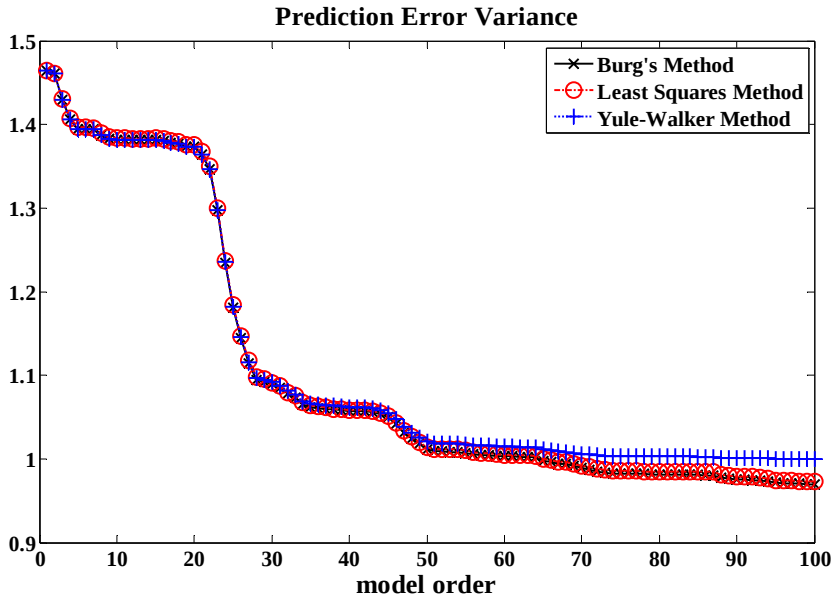

Figure 3.8: Estimated prediction error variances of three model parameter estimation methods with the maximal order of 100, in the case of mutually correlated ambient inputs and the baseline state of building structure.

In the same way, four order selection criteria, the Final Prediction Error Criterion (FPE), the Akaike Information Criterion (AIC), the Bayesian AIC (BIC) and the Schwarz Bayesian Criterion (SBC), have been evaluated. The prediction error variances were calculated by using the Burg's method. For comparing the different model orders, the models with a maximal order of 50 are estimated.

Figure 3.9 plots an example of the results of optimal order selection by four criteria. Decided by the local minimum of the relative error variances, four criteria give the same results of optimal model order of 2, as shown in Table 3.3.

Furthermore, various AR models of acceleration signals from different masses in different damage scenarios have been evaluated. Almost all the criteria give the same optimal order of 2. Therefore, the order of 2 is selected for both model estimation and distance measure.

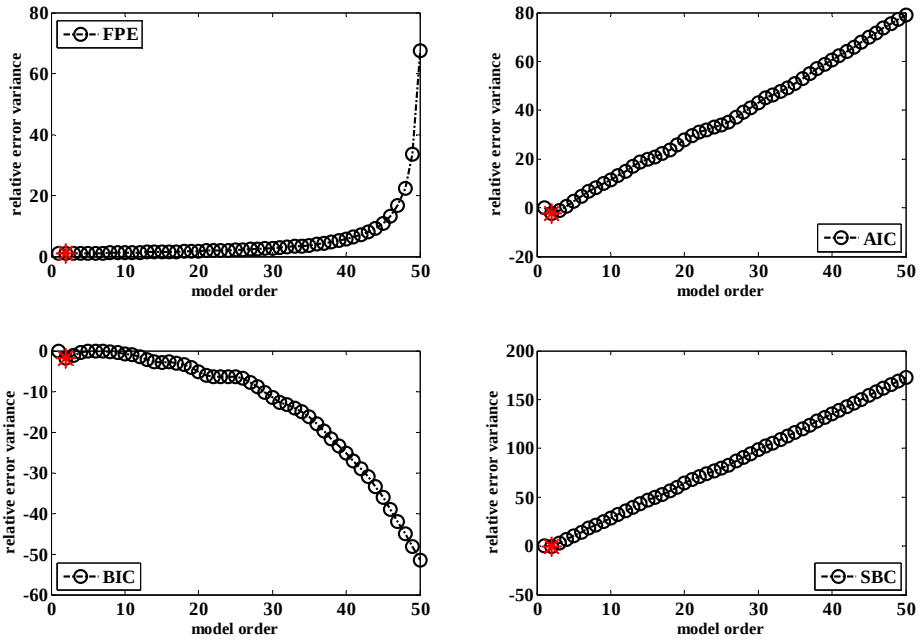

Figure 3.9: Optimal model order selected by the FPE, AIC, BIC and SBC criteria, with the maximal order of 50, in the case of mutually correlated ambient inputs and the baseline state of building structure.

Table 3.3: Optimal orders selected in the case of mutually correlated ambient excitations

Criterion	FPE	AIC	BIC	SBC
Optimal Order	2	2	2	2

Distance measures

In the case of mutually correlated ambient inputs, the damage indicators defined as the distance measures are calculated in the same way. Following the procedure of damage detection by distance measures, depicted in Figure 3.3, the distance measures between AR models are defined as the damage indicators for damage detection. Due to the optimal order selection criteria, the first two AR parameters are used to calculate the distance measures of AR models, either by (3.1.11) or (3.1.28).

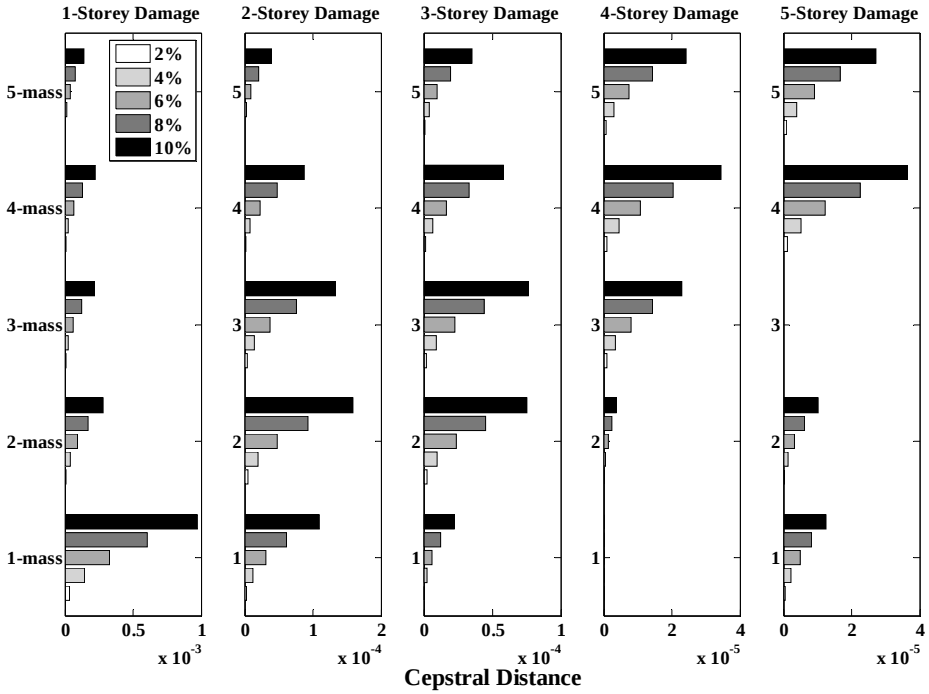

Figure 3.10: Cepstral distances in the case of mutually correlated ambient inputs.

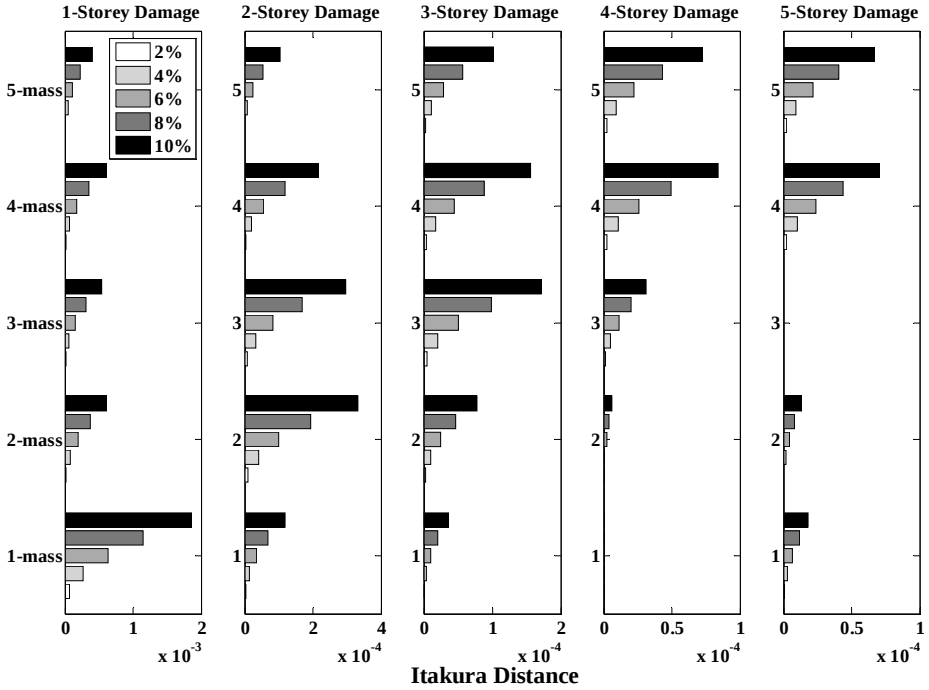

Figure 3.11: Itakura distances in the case of mutually correlated ambient inputs.

Various AR models of acceleration signals from different masses in different damage scenarios have been evaluated. Almost all the criteria give the same optimal order of 2. Therefore, the order of 2 is selected for both model estimation and distance measure. Figure 3.10 and Figure 3.11 show the results of cepstral distance measures and Itakura distance measures, respectively for the 25 damage scenarios. Similar results were obtained from the two distance measures.

It is observed from both figures that the distance measures can detect the damage by finding the changes in magnitudes, while failed in damage localization. It is difficult to identify the damage location from the distribution of the distance measure indicators. This is probably because that there are strong correlations among the multiple excitations.

It is assumed that the correlations deteriorate the ability of the distance measure to identify the damage location. Hence, to overcome the difficulty of application of distance measures to mutually correlated excitations case, it is necessary to remove the correlations, which will be discussed in the following chapter.

3.3 Summary

In this chapter, two distance measures between AR models are introduced. One is the cepstral distance, and the other is the Itakura distance. The two distance measures have been widely applied in speech recognition, neurological sequences comparison, and machine diagnostics and so on. Based on the assumption that the structural response (typically the acceleration) is seemed as the voice of structure, the feasibility of the distance measures on damage detection in civil engineering structures were investigated. For this purpose, the damage indicators were defined by the distance measures between the AR models, which are used to fit the acceleration responses from the structures.

The procedure of damage detection using the distance measure has been proposed in this chapter. Firstly, the vibration signals from building structure, acceleration time histories, are parameterized by AR models. Secondly, by using distance measures, either Itakura distance or cepstral distance, the distance between the AR models

fitting the acceleration time histories from structure in baseline state and unknown state are measured. Finally, decision can be drawn that a large distance indicators a possible damage in the structure.

Extensive numerical simulations have been carried out to evaluate the proposed damage detection method using the distance measures of AR models. The model order selection criteria, introduced in Chapter 2, were applicable to obtain the optimal orders not only for AR modeling but also distance measures. Both distance measures were calculated on the AR parameters with the orders selected by the criteria. In the mutually uncorrelated excitations case, the damage indicators succeeded in damage detection including exact damage localization. While in the mutually correlated excitations case, the damage indicators could only detect the changes in structure, but failed in identifying the damage locations. The most likely reason for this is that the correlations among the multiple outputs deteriorated the performance of damage indicators for damage localization.

Chapter 4

Pre-whitening Filter

As seen in Chapter 3, distance measures failed in damage localization when the multiple ambient excitations are mutually correlated. In practice, the excitations acting on civil engineering structures are mutually dependent and correlated, such as wind and traffic loading. To overcome this difficulty, a pre-whitening filter is applied to cancel the correlations of excitations before calculating the damage indicators.

In this chapter, we will first introduce a symmetric whitening algorithm, which is applied to remove the correlations of the input exaltations. The damage detection methodology combining the distance measure and the pre-whitening filter follows. In the end of this chapter, the effect of the pre-whitening on the damage indicator to damage location is tested on both numerical and experimental data.

4.1 Introduction of Pre-whitening Filter

The decorrelation techniques play important roles in signal processing. They are the basis for modern subspace methods of spectrum analysis and array processing and often used in a preprocessing stage in order to eliminate redundancy or to reduce noise (Cichocki et al. 2002). A whitening transform technique, the symmetric whitening algorithm is introduced here. This signal pre-processing technology is applied to pre-whiten (decorrelate) the sensor signals from vibration structure before conducting the proposed damage detection methodology.

In whitening, the m-dimension sensor signals $x(k)$ are pre-processed by using the following whitening transformation:

$$y(k) = Wx(k) \qquad (4.1.1)$$

where $y(k)$ denotes the whitened signals, and W is the $m \times m$ whitening matrix. For this purpose, the matrix W is chosen so that the covariance matrix $E\{y(k)y(k)^T\}$ becomes the unit matrix I_m. Thus the components of the whitened signals $y(k)$ are mutually uncorrelated and they have unit variance, i.e.:

$$R_{yy} = E\{yy^T\} = E\{Wxx^TW^T\} = WR_{xx}W^T = I_m \qquad (4.1.2)$$

In general, the sensor signals $x(k)$ are mutually correlated, i.e., the covariance matrix R_{xx} is a full (not diagonal) matrix. It should be noted that the matrix W is not unique, since by multiplying an arbitrary orthogonal matrix to W from the left, then a new W generates, and (4.1.2) still preserved.

Usually, since the covariance matrix of sensor signals $x(k)$ is symmetric positive definite, it can be decomposed as following:

$$R_{xx} = V_x \Lambda_x^{1/2} \Lambda_x^{1/2} V_x^T \qquad (4.1.3)$$

where V_x is an orthogonal matrix and $\Lambda_x = diag\{\lambda_1, \lambda_2, \cdots, \lambda_m\}$ is a diagonal matrix with positive eigenvalues $\lambda_1 \geq \lambda_2 \geq \cdots \geq \lambda_m > 0$. Hence, under the condition that the covariance matrix is positive definite, the required decorrelation matrix can be computed as following:

$$W = \Lambda_x^{-1/2} V_x^T = diag\left\{\frac{1}{\sqrt{\lambda_1}}, \frac{1}{\sqrt{\lambda_2}}, \cdots, \frac{1}{\sqrt{\lambda_m}}\right\} V_x^T \qquad (4.1.4)$$

or

$$W = U\Lambda_x^{-1/2} V_x^T \qquad (4.1.5)$$

where U is an arbitrary orthogonal matrix.

By substituting (4.1.3) and (4.1.4) or (4.1.5) into (4.1.2), it can be easily verified that:

$$R_{yy} = E\{yy^T\} = \Lambda_x^{-1/2} V_x^T V_x \Lambda_x V_x^T V_x \Lambda_x^{-1/2} = I_m \qquad (4.1.6)$$

$$R_{yy} = U\Lambda_x^{-1/2} V_x^T V_x \Lambda_x V_x^T V_x \Lambda_x^{-1/2} U^T = I_m \qquad (4.1.7)$$

4.2 Proposed Damage Detection Methodology

Combining the distance measure and the pre-whitening filter, the procedure of damage detection methodology is plotted in Figure 4.1:

- Firstly, the vibration signals from building structure, acceleration time histories, are pre-processed by the pre-whitening filters to remove the correlations.
- Secondly, the whitened acceleration signals are parameterized by AR models.
- Thirdly, using the distance measures, Itakura distance or cepstral distance, the distance between the AR models fitting the acceleration time histories from structure in baseline state and unknown state are measured.
- Finally, decision can be drawn that a large distance indicators a possible damage in the structure.

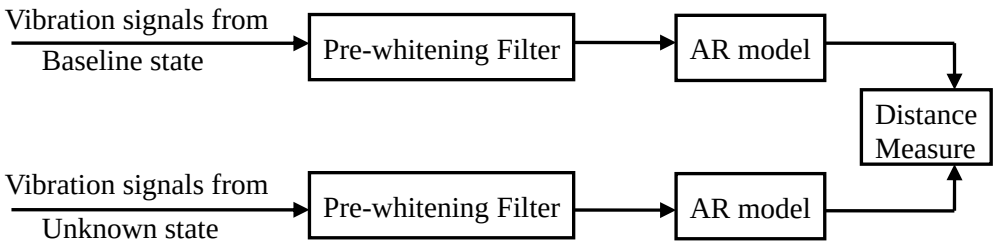

Figure 4.1: Procedure of damage detection methodology using the distance measure and the pre-whitening filter

4.3 Numerical Verification

To verify the proposed methodology combining the distance measures and the pre-whitening filters, we first give the simulation verifications on numerical data.

Figure 4.2 shows the building model used for the numerical verification. In this evaluation, the structural model is the same as that used in numerical evaluations in Section 3.2. The structural parameters of the building model, which can be referred to Section 3.2.1, are unchanged. The simplified five degree of freedom system and the output accelerations induced by the ambient forces are depicted in this figure.

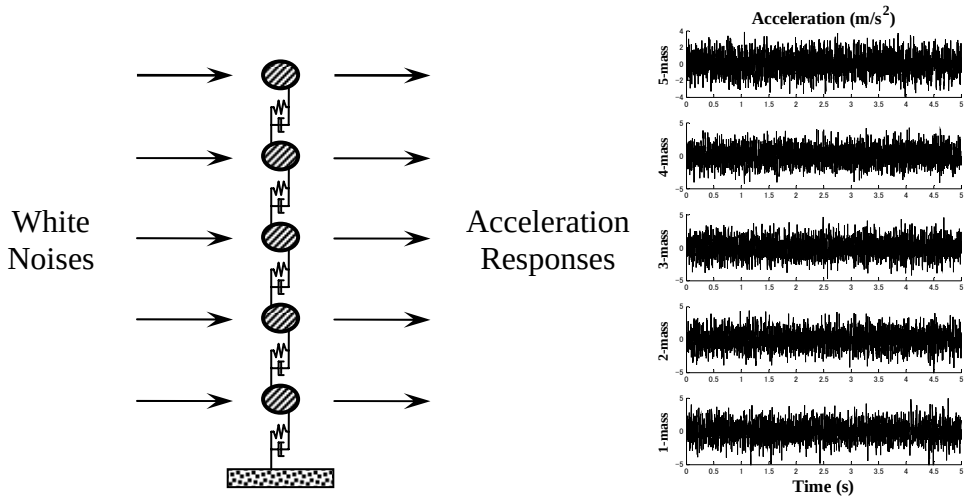

Figure 4.2: Simplified structural system and simulated acceleration time histories induced by mutually correlated ambient excitations.

In this case, we again consider the mutually correlated ambient excitations. The structural system is assumed to be subjected to five ambient excitations on every mass, which were simulated by five white noise processes. We assume the white noise processes are identical. Hence there are strong correlation among the multiple inputs and outputs, as analyzed in Section 3.2.4.

The difference between this part and Section 3.2.4 is that we here use the procedure of damage detection method, as described in Figure 4.1. In this evaluation, the acceleration time histories are pre-processed by the pre-whitening filter, before calculating the distance measures. The purpose of this step is to remove the correlations among the multiple outputs due to the mutually correlated inputs.

Covariance analysis

To observe the correlations among the inputs and outputs of the system, we give the covariance analysis by calculating the covariance matrices. For comparing with the results without using the pre-whitening filter, we used the same case as the example described in Section 3.2.4.

In section 3.2.4, we gave the covariance analysis of the input signals and the processed output signals as following:

$$R_{in} = 10^4 \times \begin{bmatrix} 0.0407 & 0.0407 & 0.0407 & 0.0407 & 0.0407 \\ 0.0407 & 0.0407 & 0.0407 & 0.0407 & 0.0407 \\ 0.0407 & 0.0407 & 0.0407 & 0.0407 & 0.0407 \\ 0.0407 & 0.0407 & 0.0407 & 0.0407 & 0.0407 \\ 0.0407 & 0.0407 & 0.0407 & 0.0407 & 0.0407 \end{bmatrix}$$

and

$$R_{out} = \begin{bmatrix} 1.6183 & 1.5043 & 1.3370 & 1.2921 & 1.2504 \\ 1.5043 & 1.8681 & 1.7529 & 1.5509 & 1.4882 \\ 1.3370 & 1.7529 & 2.0363 & 1.9457 & 1.7687 \\ 1.2921 & 1.5509 & 1.9457 & 2.2414 & 2.2205 \\ 1.2504 & 1.4882 & 1.7687 & 2.2205 & 2.6677 \end{bmatrix}$$

The covariance matrices of the input signals and the unprocessed output signals are both full matrices. Hence, to remove the correlations among the multiple outputs, the pre-whitening filter was applied on the output signals. Then, the covariance matrix of the whitened output signals is given as following:

$$R_{out\_whitened} = \begin{bmatrix} 1.0002 & 0.0000 & -0.0000 & -0.0000 & -0.0000 \\ 0.0000 & 1.0002 & -0.0000 & 0.0000 & -0.0000 \\ -0.0000 & -0.0000 & 1.0003 & -0.0000 & 0.0000 \\ -0.0000 & 0.0000 & -0.0000 & 1.0003 & -0.0000 \\ -0.0000 & -0.0000 & 0.0000 & -0.0000 & 1.0003 \end{bmatrix}$$

It can be seen that the covariance matrix of the pre-whitened output accelerations is almost a unit matrix. As a result, the correlations have been removed by using the pre-whitening filter.

(Note that the numbers in the expressions are referred to Matlab output format, in which the output display is formatted with 5 digits. This is the reason why there are numbers like -0.0000 and 0.0000).

Model analysis

In this simulation, the settings of simulation are the same as the mutually correlated excitations case, as depicted in Section 3.2.4: the length of data samples is 4001, and the sampling frequency is 200 Hz.

Based on the model parameter estimation analysis in Chapter 3, the three methods introduced in Chapter 2 are all qualified in the case of large length data samples. Since the data length of 4001 is large enough, each model parameter estimation method can be used.

By comparison, the Burg's method is the only reliable AR parameter estimation method, yielding accurate parameter estimates as well as a guaranteed stable AR model. Hereafter, the model parameters of AR models are estimated only by using the Burg's method. Figure 4.3 shows the results of estimated prediction error variances. For comparing the different model orders, the models with a maximal order of 50 are estimated.

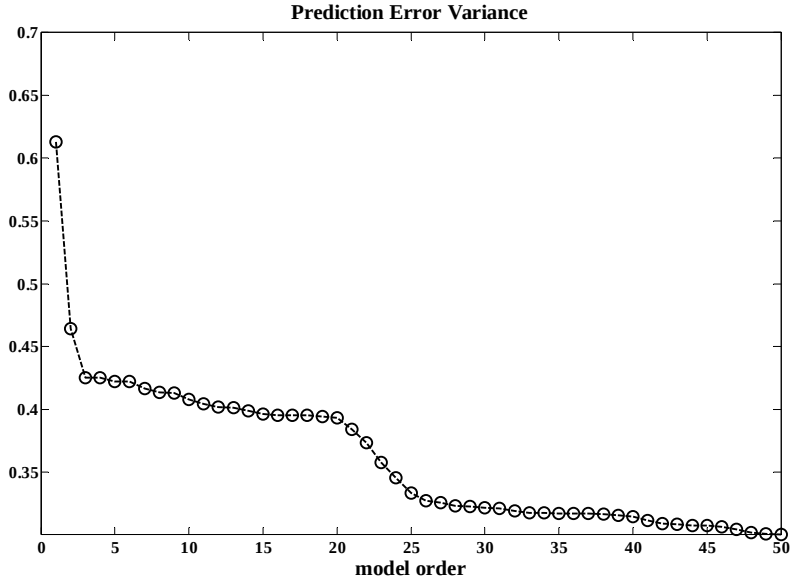

Figure 4.3: Estimated prediction error variances, with the maximal order of 50, following the pre-whitening filter, in the case of mutually correlated ambient inputs and the baseline state of building structure.

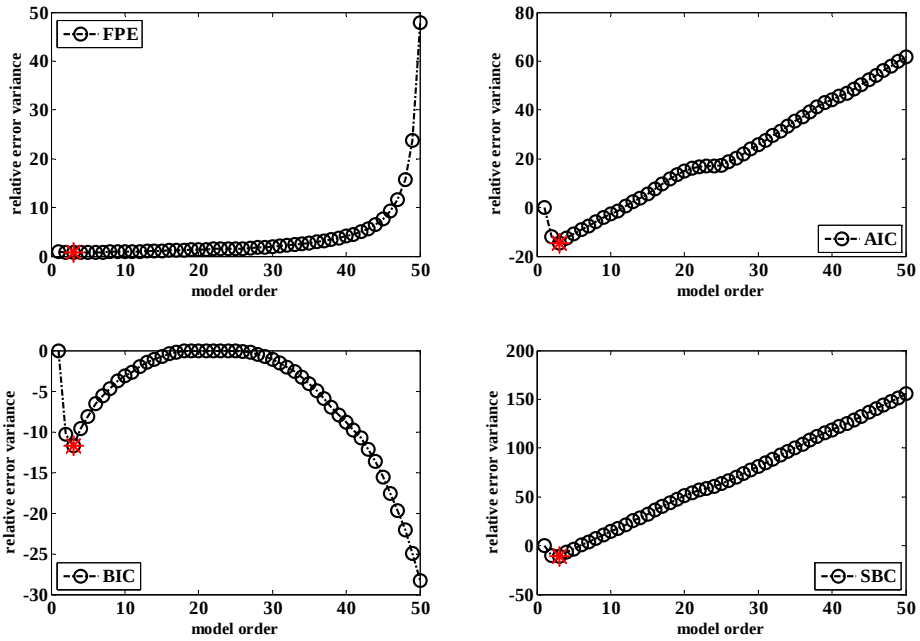

Figure 4.4: Optimal model order selected by the FPE, AIC, BIC and SBC criteria, with the maximal order of 50, following the pre-whitening filter, in the case of mutually correlated ambient inputs and the baseline state of building structure.

Table 4.1: Optimal orders selected in the case of mutually correlated ambient excitations using the pre-whitening filter

Criterion	FPE	AIC	BIC	SBC
Optimal Order	3	3	3	3

Various AR models of data samples from different masses and in different damage scenarios have been evaluated. The similar results of optimal orders were obtained.

Figure 4.4 plot the relative prediction error variances by the FPE, AIC, BIC and SBC criteria. Decided by the local minimum, the FPE, AIC, BIC and SBC criteria all give the optimal model order of 3, as shown in Table 4.1. Therefore, the order of 3 is selected to estimate the AR models and to measure the distance between AR models.

Distance measure

Figure 4.5 and Figure 4.6 show the results of cepstral distance measures and Itakura distance measures in the case of mutually correlated ambient inputs.

The procedure of damage detection using both distance measures and pre-whitening filters, as shown in Figure 4.1, was applied. It should be noted that the accelerations time histories have been passed through the pre-whitening filters before calculating the distance measures of AR models, either by (3.1.16) or (3.1.27). Due to the optimal order selection criteria, the first three AR parameters are used for model estimation and distance measure. Form the two figures, similar results show that both distance measures yield reasonable damage detection.

Compared with the results in Section 3.2.3, it is observed that two distance measures here succeed in identifying damage and its location when using pre-whitening filter. Hence by using the pre-whitening filter, the performance of distance measures, especially for damage localization, can be improved evidently. It can be concluded that the pre-whitening filter is crucial for the damage indicators when the ambient excitations are mutually correlated

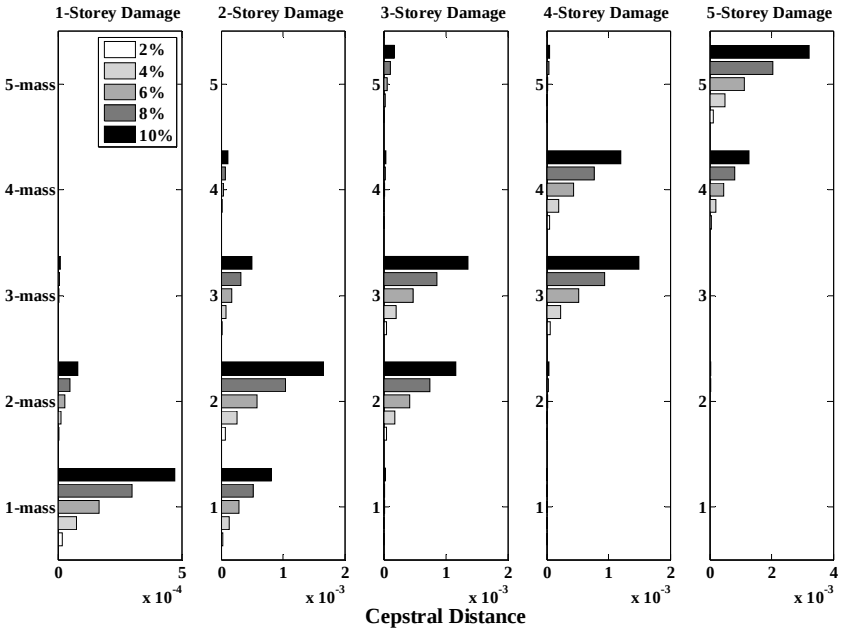

Figure 4.5: Cepstral distances, following the pre-whitening filter, in the case of mutually correlated ambient inputs.

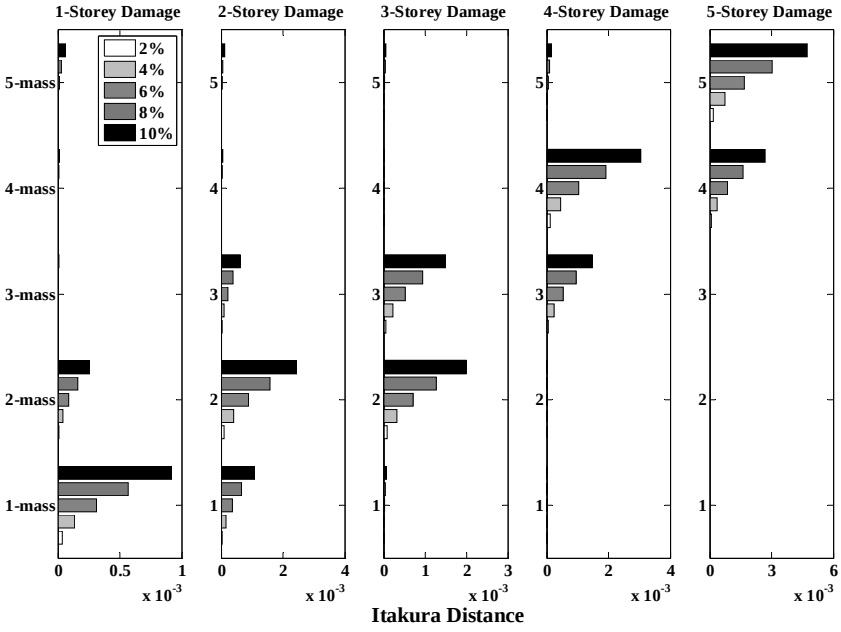

Figure 4.6: Itakura distances, following the pre-whitening filter, in the case of mutually correlated ambient inputs.

4.4 Experimental Verification

In this section, the damage detection methodology, described in Section 4.2, is evaluated on the experimental data. The structural responses were gathered from a shake table test, which was conducted by the Building Research Institute of Japan (2004). The experimental building model is depicted in Figure 4.7. The experiment data have been used in Chapter 2 for evaluating the model parameter methods and model order selection criteria of AR models.

The weight of every storey is 2.57 ton and storey heights are all 1 m. The length of long-side is 3 m, while that of the short-side is 2 m. The excitation of test is a white noise with bandwidth of 0~200 Hz generated by the vibration exciter, along the long-side direction. On every storey of structure the accelerometers were mounted on both long-sides to record the acceleration responses along the long-side direction. The acceleration time histories were recorded with the sampling period 0.005 sec, for 40.92 sec. Thus each record has 8,192 sampled data.

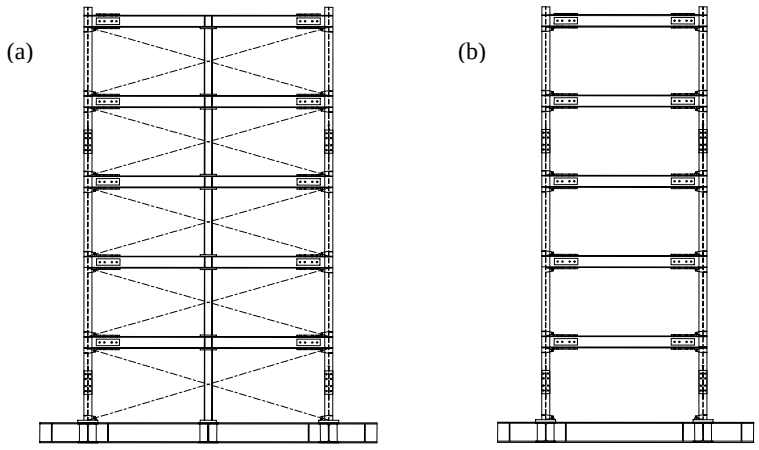

Figure 4.7: Experimental building model: (a) long-side; and (b) short-side.

As depicted in Figure 4.7, the test structure model is a five-storey steel structure. Figure 4.7 (a) and Figure 4.7 (b) show the long-side and short-side of the structure, respectively. As the original state, the central columns and braces on the long-side have been installed on every storey. To evaluate the damage scenarios, the members of structures were removed step by step.

The five storey building structure model can be simplified as a five degree of freedom system. Figure 4.8 plots the diagram of the simplified five degree of freedoms system of the experiment building model along the long-side, and the acceleration records measured by the accelerometers installed on the model. Since the accelerometers were all mounted on the long-side and the members on the long-side were removed to simulate the damage scenarios, the long-side of the structure will be considered only.

As shown in the left part of the figure, the excitation was acted on the base of the building model, which is mounted on the shake table. The structure was excited by the vibration exciter on the shake table. The measured acceleration outputs were plotted in the right part of the figure.

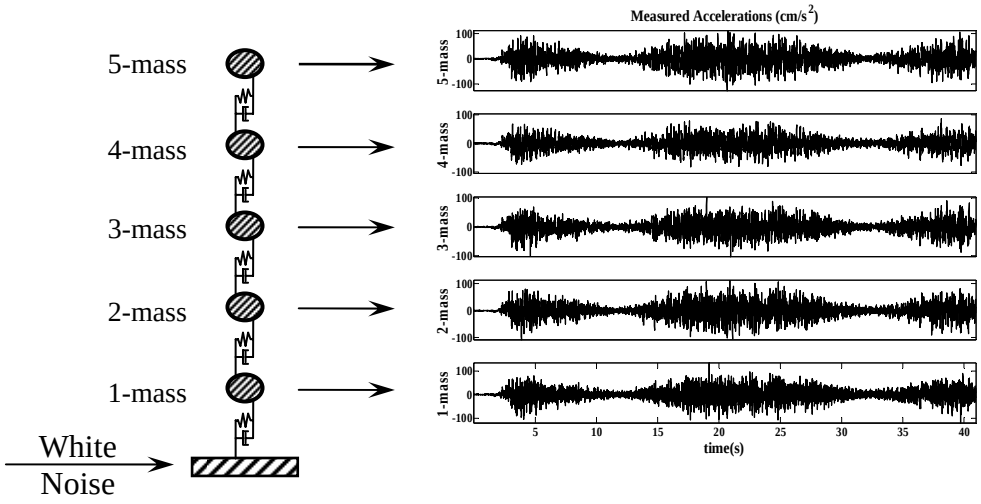

Figure 4.8: Simplified structural system of the experiment building model and acceleration time histories induced by vibration exciter at the shake table.

The mode characteristics of this experimental building model, including the natural frequencies and damping ratios of the original structure, have been identified using Auto-Regressive eXogenous (ARX) model by Yoshimoto et al. (2002).

Figure 4.9 shows the Bode plot of the identified ARX model. The sharp peaks appearing in the power spectrum indicate the strong structural resonances, i.e. natural frequencies in the structure.

The mode characteristics of the building model including natural frequencies and damping ratios were identified, as shown in Table 4.2.

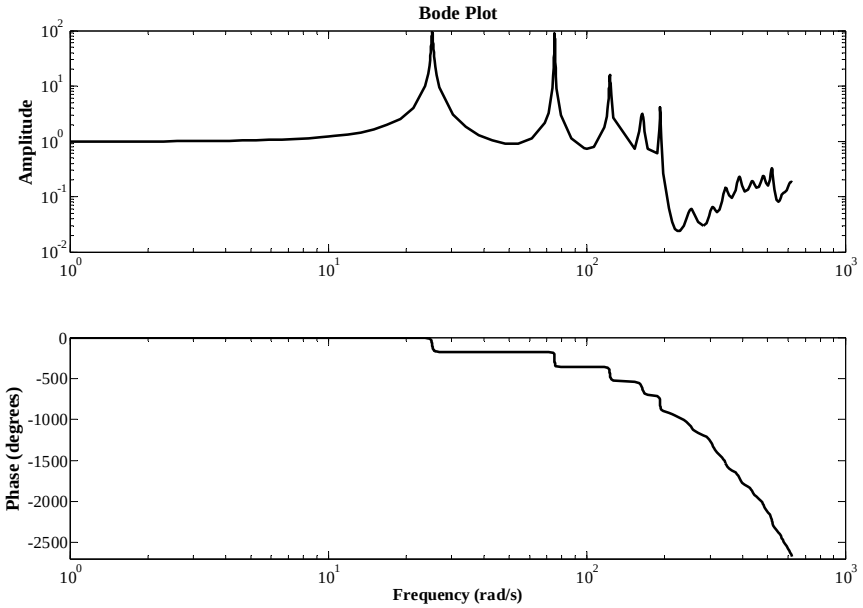

Figure 4.9 : Bode plot of identified experimental building model.

Table 4.2: Mode characteristics of experimental building model.

Mode	Natural Frequency (Hz)	Damping Ratio (%)
1	4.00	1.16
2	11.98	0.15
3	19.56	0.32
4	26.05	0.30
5	30.47	0.08

Covariance analysis

The building model is subjected to base excitation with white noise inputs. Although the structural system is a single-input-multiple-output (SIMO) model, the excitations can be equivalently seemed as five inertial forces acting on every mass.

We give an example of the covariance matrix of the multiple outputs and the pre-whitened acceleration outputs as follows:

$$R_{out} = \begin{bmatrix} 519.5391 & 313.9641 & 92.7655 & -15.4881 & -102.7812 \\ 313.9641 & 625.8951 & 272.5041 & -22.7911 & -126.4825 \\ 92.7655 & 272.5041 & 458.3612 & 174.0306 & -82.6457 \\ -15.4881 & -22.7911 & 174.0306 & 379.3122 & 214.4413 \\ -102.7812 & -126.4825 & -82.6457 & 214.4413 & 724.3434 \end{bmatrix}$$

and

$$R_{out\_white} = \begin{bmatrix} 1.0003 & 0.0000 & -0.0000 & 0.0000 & -0.0000 \\ 0.0000 & 1.0003 & -0.0000 & -0.0000 & 0.0000 \\ -0.0000 & -0.0000 & 1.0003 & 0.0000 & 0.0000 \\ 0.0000 & -0.0000 & 0.0000 & 1.0002 & -0.0000 \\ -0.0000 & 0.0000 & 0.0000 & -0.0000 & 1.0003 \end{bmatrix}$$

From the covariance matrix of the measured outputs R_{out}, we know that there are mutual correlations among the multiple outputs. Hence, the pre-whitening filter is also required in this case. Before calculating the distance measures, the acceleration time series were pre-processed by the pre-whitening filter to cancel the correlation. By passing the pre-whitening filter, the covariance matrix of the pre-whitened outputs $R_{out\_measure}$ becomes a unit matrix.

Model analysis

In Chapter 2, the acceleration time histories from this experiment have been used for AR model analysis. Three different lengths of data samples have been evaluated for various methods. For calculating the distance measures, the even larger length of data samples are used. The various lengths of data samples have been tried, it is found that the length of data sample, if larger than a definite value (about 400), does not affect the AR model on the parameter estimation, and also on the distance measures.

Next, we give an example of the results on AR parameterization and order selection. The length of data sample is 4001, as shown in Figure 4.10. For example, the accelerations from the fifth storey were selected for model analysis. Figure 4.11 shows the results of the prediction error variances.

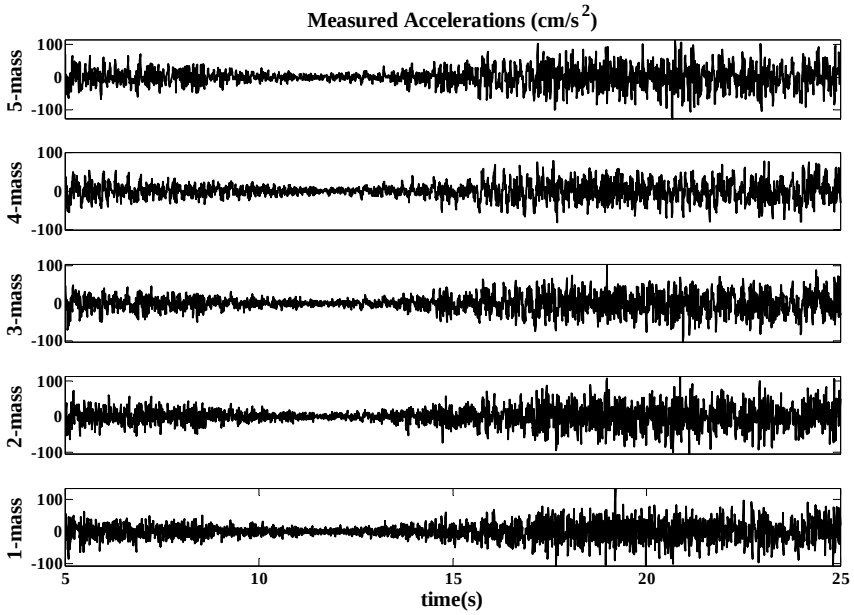

Figure 4.10: Accelerations sections of 4001 data samples ([5 25] second) Measured from shake table test

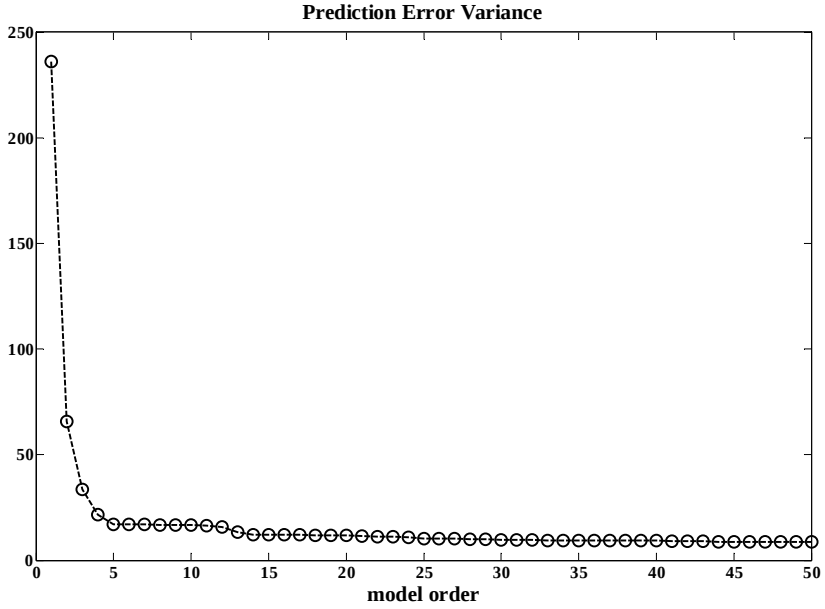

Figure 4.11: Estimated prediction error variances, following the pre-whitening filter, with the maximal order of 50, in the case of shake table excitations and the baseline state of building structure.

Figure 4.12 plots the relative prediction error variances by the FPE, AIC, BIC and SBC criteria respectively. All the criteria give the optimal order of 5, as shown in Table 4.3.

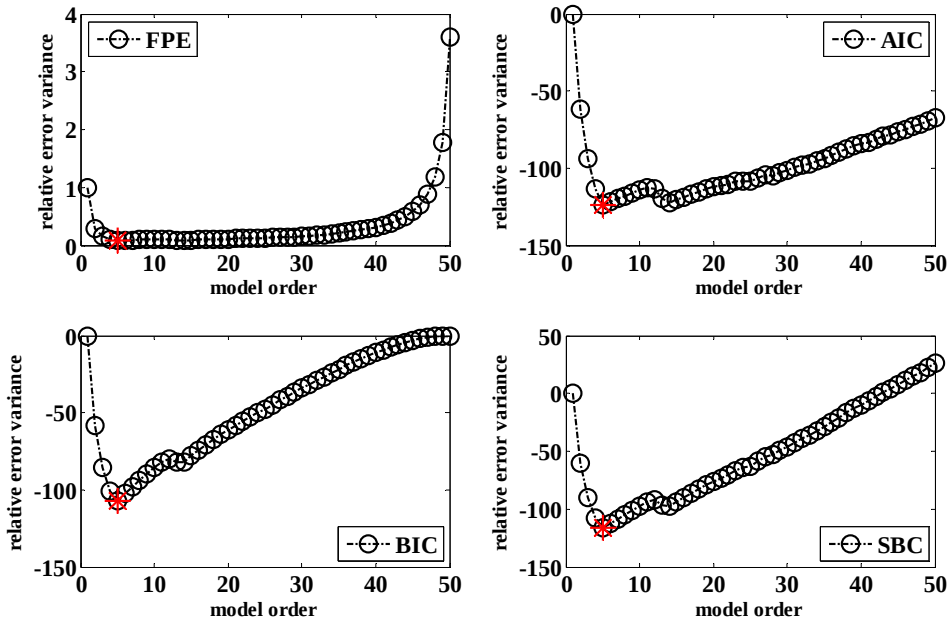

Figure 4.12: Optimal model order selected by the FPE, AIC, BIC and SBC criteria, following the pre-whitening filter, with the maximal order of 50, in the case of shake table excitations and the baseline state of building structure.

Table 4.3: optimal orders selected in the case of shake table test.

Criterion	FPE	AIC	BIC	SBC
Optimal Order	5	5	5	5

The optimal orders selected by four criteria are the same as the case of large length case (length of 401) in Section 2.4.2, as shown in Figure 2.17. The results imply that the data samples with the length of 401 are large enough for the AR models fitting of the accelerations from the shake table tests.

4.4.1 Removing of Columns Case

Assume the structural damages scenarios are simulated by removing the members of the building model, such as the columns and braces. In this experiment, the members on the long side of the building model were removed step by step. As a result, the corresponding inter-storey stiffness was reduced. The purpose of the damage indicator defined as the distance measures is to find the location where the inter-storey stiffness decreased.

In the first stage, the central columns, on both long sides of the building model, were removed. Three damage scenarios have been considered: the central column on the first, third and fifth storey was removed respectively, as shown in Figure 4.13 (a), (b) and (c). To distinguish the different AR models fitting the acceleration outputs from the structure model in various states, the original structure with full central columns and braces, as shown in Figure 4.14, is referred as the baseline state. The unknown states are referred to the three damage scenarios by removing the columns on different storeys.

Following the damage detection procedure depicted in Figure 4.1, the measured acceleration time histories were passed through the pre-whitened filters, and then the distance measures between the baseline state and the three damage scenarios were calculated.

It is noted that the optimal order of AR modeling, 5 obtained by the criteria, does not yield reasonable damage detection results, while the order of 2 or 3 can yield ideal results. In the most numerical evaluations, the order selection criteria give the optimal orders both for AR modeling and distance measures. However, the order selection criteria should be carefully used in experimental environment or real application.

Two distance measures, Itakura distance measure and cepstral distance measure were both evaluated. Figure 4.15 and Figure 4.16 plot the results for both distance measures without using the pre-whitening filters, and Figure 4.17 and Figure 4.18 plot the results following the pre-whitening filters.

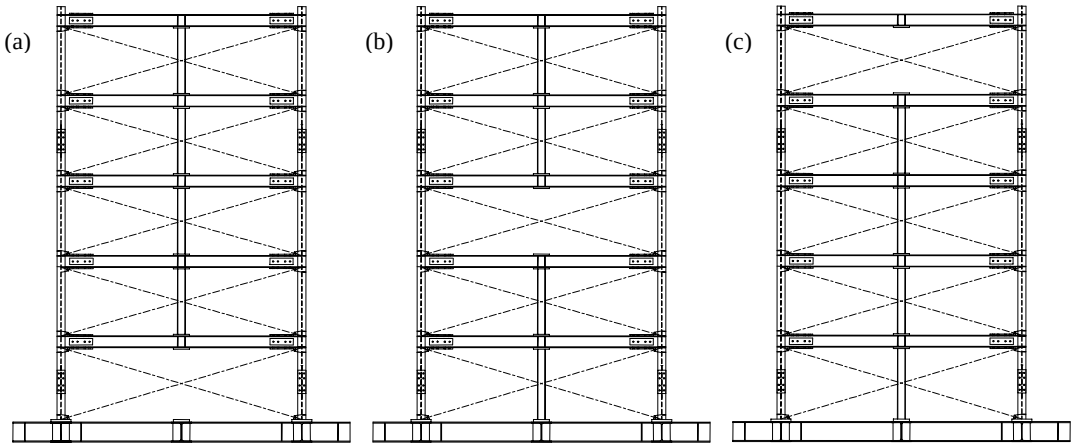

Figure 4.13: Damage scenarios by removing the central columns along the both long-sides on the (a) first; (b) third; and (c) fifth storey.

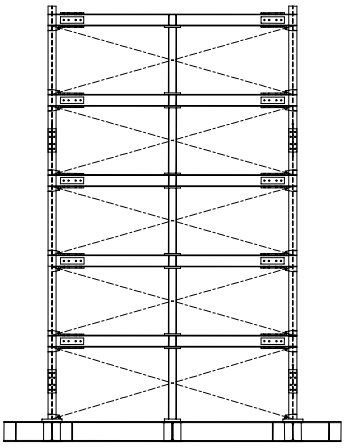

Figure 4.14: Baseline state of structure in the case of damage scenarios by removing the central columns on the both long-sides

As shown in Figure 4.15 and Figure 4.16, it is seen that without pre-whitening filter, both distance measures failed in damage localization. On the contrary, it is seen in Figure 4.17 and Figure 4.18 that the distance measures of the damaged inter-storeys, where the columns have been removed, are clearly larger than those of other storeys. For each damage scenario, the damage indicators are capable of identifying the possible damage location.

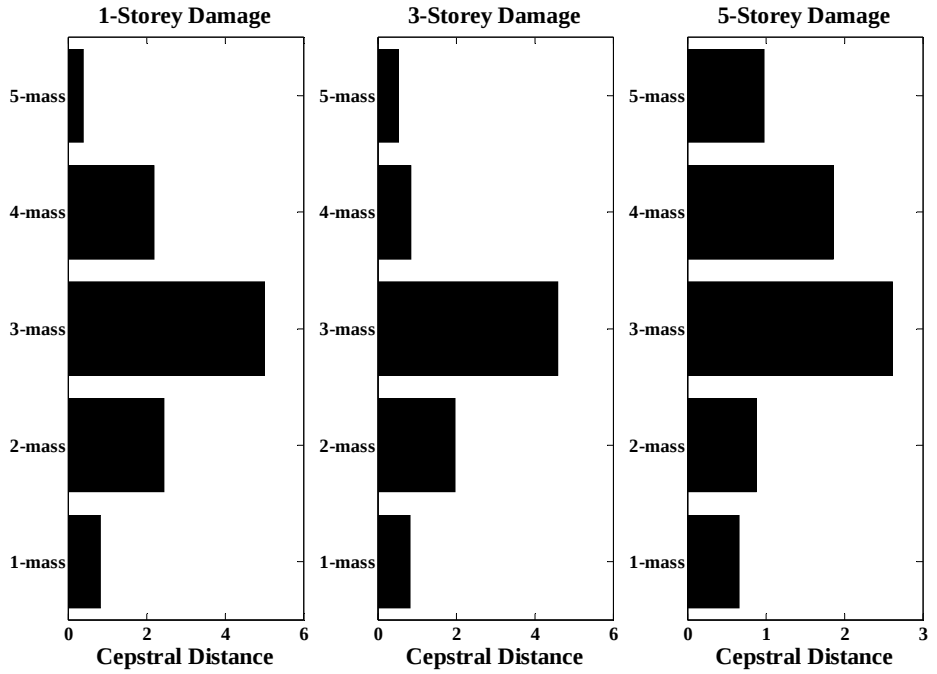

Figure 4.15: Cepstral distances, without the pre-whitening filter, in the case of shake table test and removing the central columns.

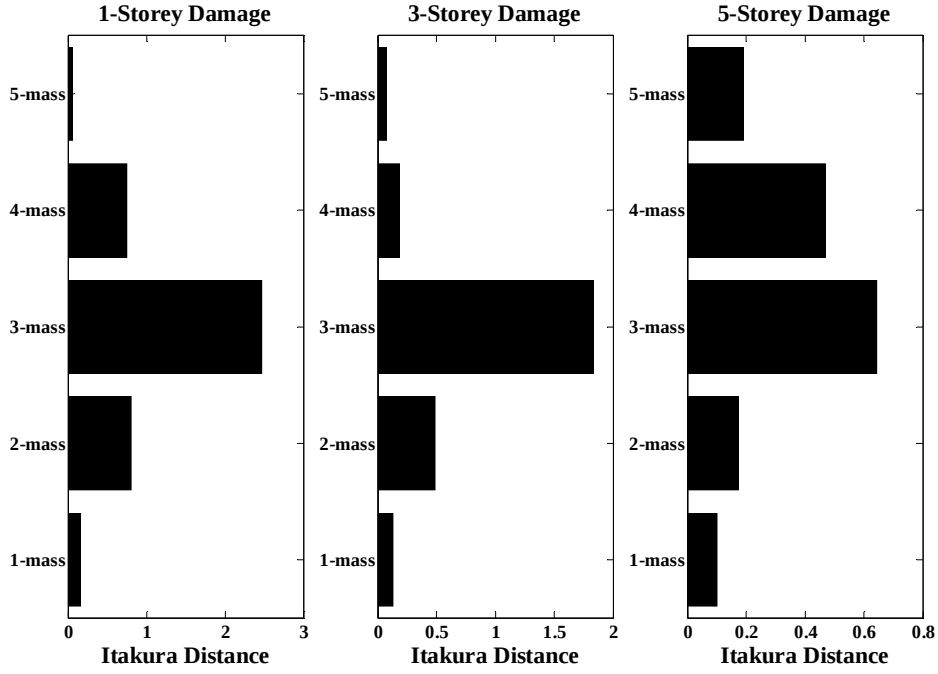

Figure 4.16: Itakura distances, without the pre-whitening filter, in the case of shake table test and removing the central columns.

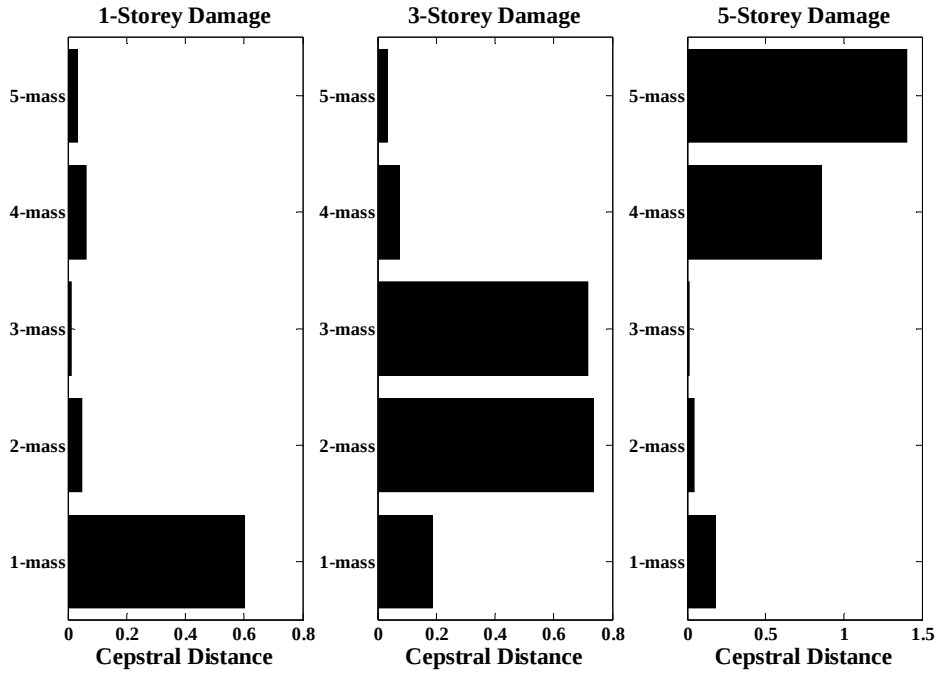

Figure 4.17: Cepstral distances, following the pre-whitening filter, in the case of shake table test and removing the central columns.

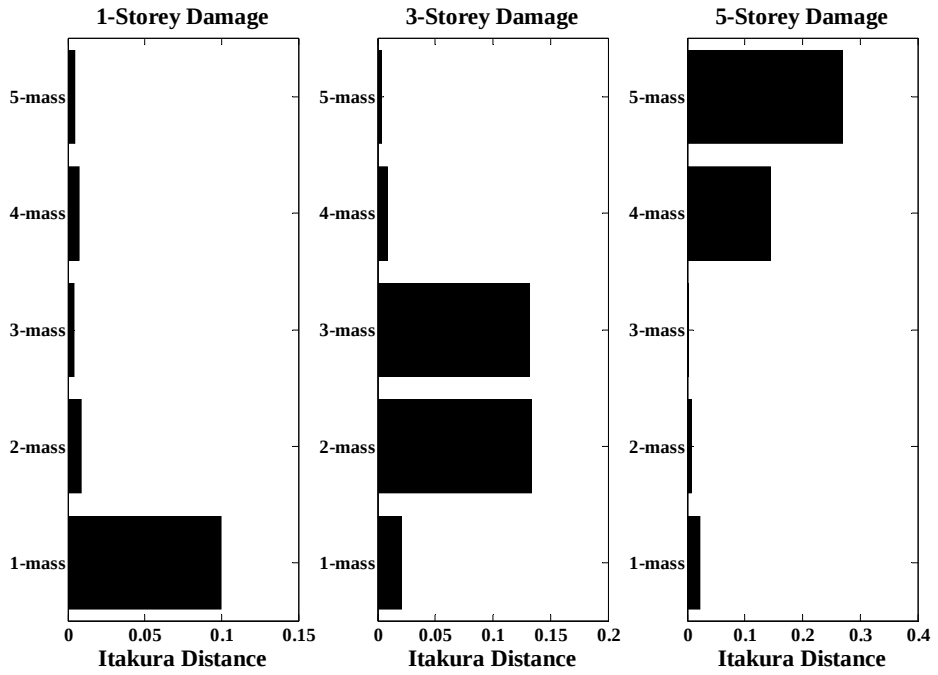

Figure 4.18: Itakura distances, following the pre-whitening filter, in the case of shake table test and removing the central columns.

4.4.2 Removing of braces

In the second stage, the braces on both long sides of the building model were further removed. Three damage scenarios have been considered: the braces on the first, third and fifth storey was removed respectively, as shown in Figure 4.19 (a), (b) and (c). In this case, the structure with full braces, as shown in Figure 4.20, is referred as the baseline state. The unknown states are referred to the three damage scenarios by removing the brace on different storeys.

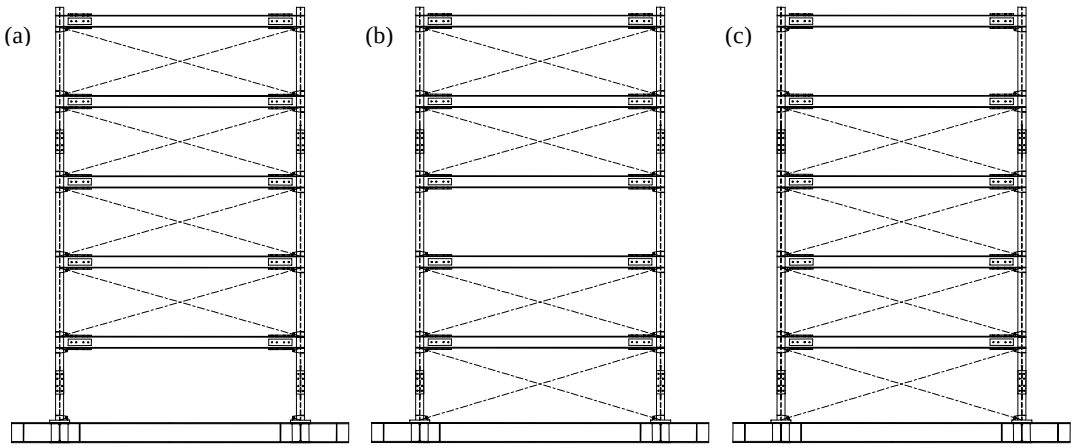

Figure 4.19: Damage scenarios by removing the braces along the both long-sides on the (a) first; (b) third; and (c) fifth storey.

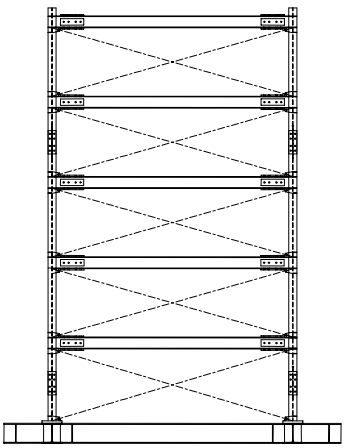

Figure 4.20: Baseline state of structure in the case of damage scenarios by removing the braces on the both long-sides.

Figure 4.21: Cepstral distances, without the pre-whitening filter, in the case of shake table test and removing the braces.

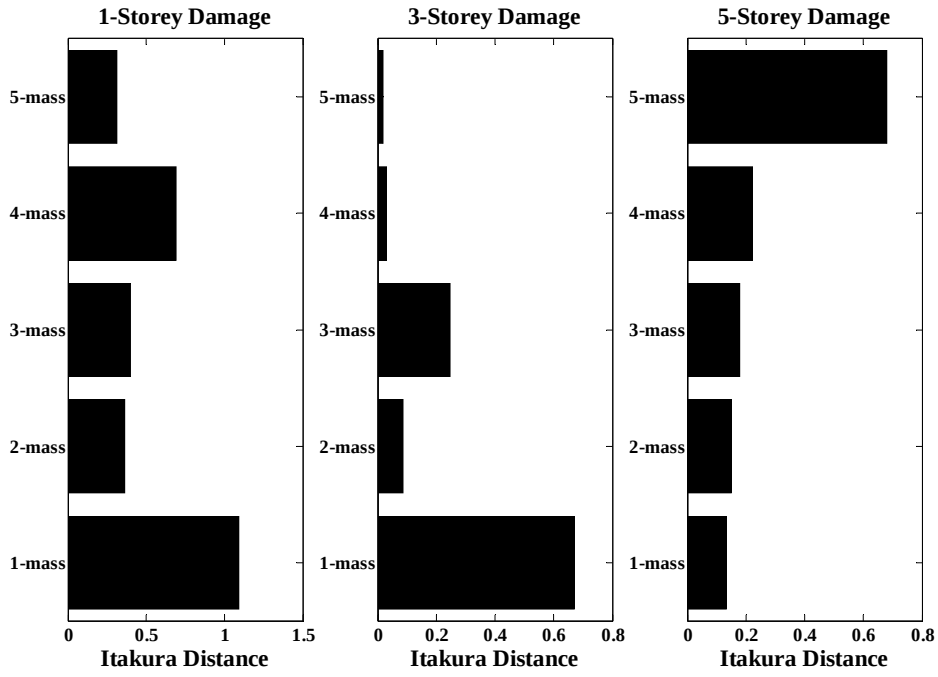

Figure 4.22: Itakura distances, without the pre-whitening filter, in the case of shake table test and removing the braces.

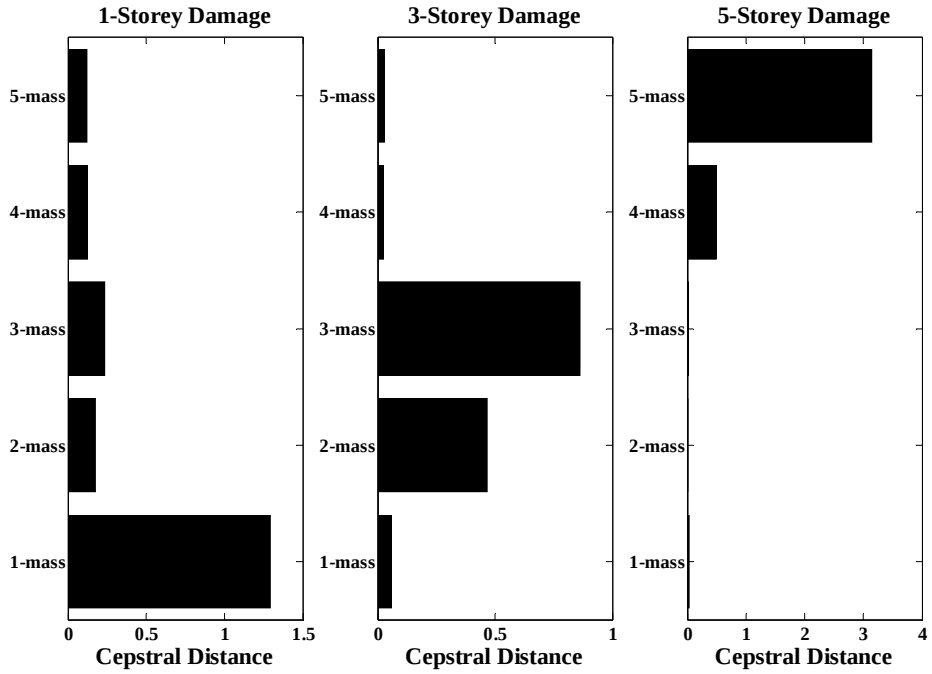

Figure 4.23: Cepstral distances, following the pre-whitening filter, in the case of shake table test and removing the braces.

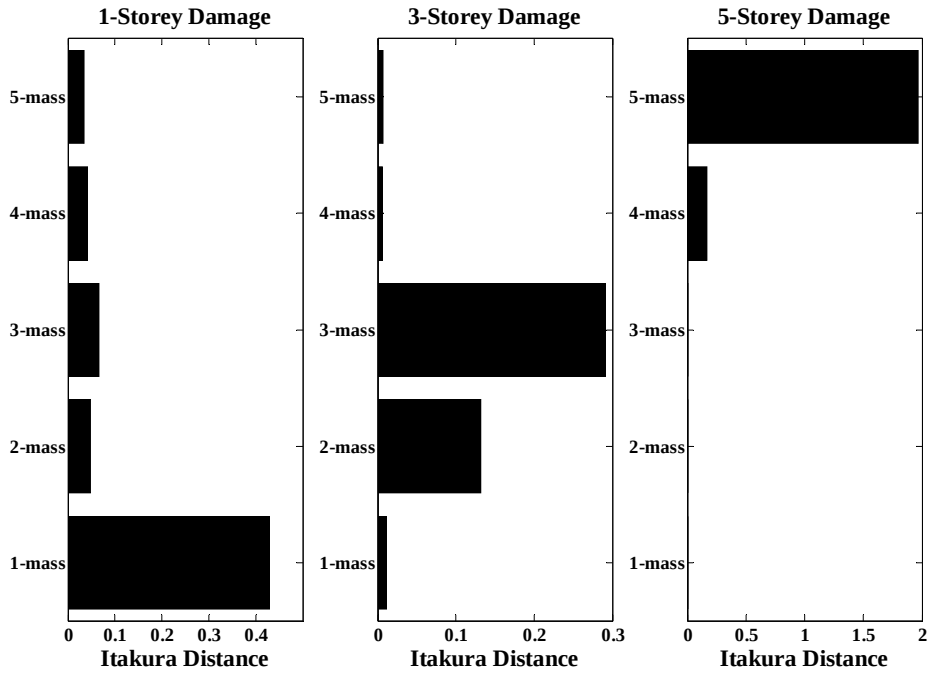

Figure 4.24: Itakura distances, following the pre-whitening filter, in the case of shake table test and removing the braces.

Similarly, the damage detection procedure depicted in Figure 4.1 was applied to obtain the distance measures between the baseline state and the three damage scenarios. Two distance measures, Itakura distance measure and cepstral distance measure were also both evaluated.

When evaluating the distance measures on damage detection using various AR parameter orders, the discrepancy of order selection between AR modeling and distance measure also occurs. It is found again that, the optimal order of AR modeling, 5 obtained by four order selection criteria, does not yield reasonable damage detection results, while the order of 2 or 3 can yield ideal results.

Figure 4.21 and Figure 4.22 plot the results for both distance measures without using the pre-whitening filters, and Figure 4.23 and Figure 4.24 plot the results following the pre-whitening filters. From the results as shown in the figures, it can be concluded that both the distance measures are qualified for damage localization with the benefits of pre-whitening filters.

4.3 Summary

This chapter has discussed the effect of the pre-whitening filter on distance measure for damage detection. In civil engineering applications, the multiple excitations acting on the structure are mutually correlated, thus result in correlations among the multiple outputs. The performance of the damage indicators, defined as the distance measures either the cepstral distance or the Itakura distance, however, are deteriorated evidently when the structure is subjected to mutually correlated excitations. Therefore, it is crucial to remove the correlations for application of the distance measures. For this purpose, the pre-whitening filter is required to make the multiple outputs mutually uncorrelated with each other.

Combining the distance measures introduced in Chapter 3 with the pre-whitening filter introduced in this chapter, a damage detection methodology has been proposed in Section 4.2. Both numerical and experimental evaluations have been given to evaluate the proposed methodology. Each evaluation compared the results of distance

measures by using and without using the pre-whitening filters. It can be concluded that the pre-whitening filter is crucial for the distance measures to carry out damage detection, especially for damage localization.

When estimating the AR models, the three parameter estimation methods introduced in Chapter 2 are all qualified for the large length data samples. The performances of three methods only diverge for the small data samples. In all the simulations of this chapter, the Burg's method is selected because of its accuracy and stability. Another important issue of distance measure using AR parameters is the order selection. In most of the numerical verifications, the order selection criteria for AR model estimation are also applicable to distance measures. However, when evaluating the experimental data of the shake table test, using the optimal order for the AR modeling, the distance measures does not yield the reasonable damage detection results. A little lower order than the optimal order for AR modeling seems more reasonable for distance measure. Therefore, the order selection for distance measure, especially for real measurements, should be further carefully investigated.

Chapter 5

Conclusion and Perspective

5.1 Conclusion

In this thesis, we have proposed the damage detection method using AR model and its distance measures and the pre-whitening filters.

Three parameter estimation methods and order selection criteria of AR modeling have been evaluated on the acceleration measurements from a shake table test. Results indicate that, in the case of the short data length, the Yule-Walker method does not perform as good as the Burg' method and the least squares method. They are all qualified for AR modeling when deal with the data samples with large length. By comparison, the Burg's method behaves well on both correctness and stability. Therefore, in the following chapters, the Burg's method was used as the default method. In addition, four model selection criteria, such as FPE, AIC, BIC and SBC have also been evaluated. Although the nearly same results were obtained by four criteria in the case of Chapter 2, the disagreements on optimal order selection occurred in the later chapters. Relatively, the FPE and AIC gave more correct orders than the BIC and SBC.

The distance measures, either the cepstral distance or the Itakura distance, were introduced in Chapter 3. The proposed damage detection method used the distance measures of AR models as the damage indicators. The performance of the proposed damage indicators have been tested on some numerical simulations. It was found that the model order selection criteria, introduced in Chapter 2, yielded optimal orders not only for AR modeling but also distance measures. Dealing with the AR parameters with selected orders, the damage indicators were obtained by either distance measure.

Results indicated that both distance measures are qualified for damage detection including exact damage localization in the case of mutually uncorrelated excitations. Results also indicated that in the case of mutually correlated excitations, the distance measures failed in damage localization. This probably results from that the correlations among the multiple outputs affect the damage indicators on damage localization. The cancellation of the mutual correlations is therefore required.

We proposed using the pre-whitening filter for removing the correlations in Chapter 4. Combining the distance measures with the pre-whitening filter, a damage detection methodology was proposed then. To evaluating the proposed methodology, numerical and experimental data have been both tested. Results indicated that the pre-whitening filter is crucial for the distance measures to carry out damage detection, especially for damage localization. From the evaluations, it was found that for the large length data samples the three parameter estimation methods introduced in Chapter 2 are all qualified for AR modeling. Relatively, we preferred the Burg's method because of its accuracy and stability. The AIC and FPE criteria also performed better and stable than the BIC and SBC. However, it should be noted that when dealing with the experimental data from the shake table test, the order selected by the above criteria could not yield the reasonable results, while a relatively little lower order gave clear information of damage locations.

5.2 Perspective

We here discuss some limitations and unresolved problems of the proposed method.

The various current damage detection methods are hard to estimate the damage severity. The method in this work is not exception. Although the evaluation examples have shown that the distance measures increase monotonically with damage severity, which provides the potential to damage quantification, it's early to say it can estimated the severity of damage. The accurate relationship between the damage indicator and damage severity should be further investigated carefully.

In essence, the distance measures used in this work are related to the SISO model. Although we have treated the correlations associated with the MIMO model by

introducing the pre-whitening filter, the best solution is expected to utilize the distance measures of the MIMO model. Recently, a definition of distance for multiple Gaussian processes has been presented by Boets et al. (2007).

The optimal order selection is still a difficult problem. The order selection for the AR modeling and the distance measures seems not to be the same topic. We guess that the uncertainty in excitations or the measurement noise results in the divergence between order selection for AR modeling and distance measures. Although the order selection criteria for AR modeling can be a reference to distance measure, the use of the selected order should be very careful.

In addition, either the numerical simulation or the shake table test was performed on the simple models, which in practice is far away from the reality. In reality, the facts of measurement noise and nonstationary input should be considered. The basis of this method should include an accurate baseline AR model of original and safe structure, which is also a hard task for a complex structure. Hence, to fully evaluate the proposed method, more investigations on the complex structure and field experiments should be conducted.

Reference

1. Akaike, H., 1969, Fitting autoregressive models for prediction, *Annals of the Institute of Statistical Mathematics*, 21, 243–247.

2. Akaike, H., 1974, A new look at the statistical model identification, IEEE *Transaction on Automatic Control*, 19, 716-723.

3. Akaike, H., 1979, A Bayesian extension of the minimum AIC procedure of autoregressive model fitting, *Biometrika*, 66.

4. Alvandi, A. and Cremona, C., 2006, Assessment of vibration-based damage identification techniques, *Journal of Sound and Vibration*, 292 (1), 179–202.

5. Basseville, M., 1989, Distance measures for signal processing and pattern recognition, *Signal Processing*, 18(4), 349–369.

6. Basseville, M., Abdelghani, M. and Benveniste, A., 2000, Subspace-based fault detection algorithms for vibration monitoring, *Automatica*, 36 101-109.

7. Berryman, J. G., 1978, Choice of operator length for maximum entropy spectral estimation, *Geophysics*, 43, 1384-1391.

8. Bissacco, A., Chiuso, A., Ma, Y. and Soatto, S., 2001, Recognition of human gaits, *Proceeding of the IEEE International Conference on Computer Vision and Pattern Recognition*, 401-417.

9. Boets, J., De Cock, K., Espinoza, M. and De Moor, B., 2005, Clustering time series, subspace identification and cepstral distances, *Communications in Information and Systems*, Special Issue Dedicated to the 70th Birthday of Thomas Kailath, Part I, 5(1), 69-96.

10. Boets, J., De Cock, K. and De Moor, B., 2006, Distances between dynamical models for clustering time series, *Proceeding of the 14th IFAC Symposium on System Identification (SYSID-2006)*, Newcastle, Australia, 392-397.

11. Boets, J., De Cock, K. and De Moor, B., 2007, A mutual information based distance for multivariate Gaussian processes, *Lecture Notes in Control and Information Sciences*, 364. 15-33.

12. Bogert, B. P., Healy, M. J. R. and Tukey, J. W., 1963, The quefrency alanysis of time series for echoes: cepstrum, pseudo-autocovariance, cross-cepstrum, and saphe cracking, *Proceedings of the Symposium on Time Series Analysis (M. Rosenblatt, Ed).* Wiley: New York, 1963; 209-243.

13. Brockwell, P. J. and Davis, A., 1991, *Time Series: Theory and Methods*. 2nd ed. Springer-Verlag, New York, NY.

14. Building Research Institute of Japan, 2004, *Guidelines for Structural Health Monitoring of Buildings and its Application*, ISSN 0451-6486, 142, 78-83.

15. Burg, J. P., 1975, *Maximum Entropy Spectral Analysis*, Ph.D. dissertation, Stanford University, Stanford CA.

16. Carden, E. P. and Fanning, P., 2004, Vibration based condition monitoring: a review, *Structural Health Monitoring*, 3(4), 355-377.

17. Chang, P.C., Flatau, A. and Liu, S. C., 2003a, Review paper: health monitoring of civil infrastructure, *Structural Health Monitoring*, 2(3), 257-267.

18. Chang, P.C. and Liu, S. C., 2003b, Recent research in nondestructive evaluation of civil infrastructures, *Journal of Materials in Civil Engineering*, 15(33), 298-304.

19. Cichocki, A. and Amari, S., 2002, *Adaptive Blind Signal and Image Processing*, John Wiley & Sons: West Sussex, 130-175.

20. Davis, S. B. and Mermelstein, P., 1980, Comparison of parametric representations for monosyllabic word recognition in continuously spoken sentences, *IEEE Transaction on Acoustics, Speech, and Signal Processing*, 28(4), 357–366.

21. De Cock, K., 2002a, *Principal Angles in System Theory, Information theory and Signal Processing*, PhD thesis, K. U. Leuven, Faculty of Applied Sciences, Leuven, Belgium.

22. De Cock, K. and De Moor, B., 2002b, Subspace angles between ARMA models, *Systems & Control Letters*, 46(4), 265–270.

23. De Cock, K., Hanzon, B. and De Moor, B., 2003, On a cepstral norm for an ARMA model and the polar plot of the logarithm of its transfer function, *Signal Processing*, 83(2), 439–443.

24. De Cock, K. and De Moor, B., 2004, A conjecture on Lyapunov equations and principal angles in subspace identification, *Unsolved Problems in Mathematical Systems and Control Theory*, 287–292. Princeton University Press, Available on http://pup.princeton.edu/math/blondel/.

25. De Hoon, M. J. L., Van Der Hagen, T. H. J. J., Schoonewelle, H., Van Dam, H., 1996, Why Yule−Walker should not be used for autoregressive modeling, *Annals of Nuclear Energy*, 23 (15), 1219−1228.

26. De Lautour, O.R. and Omenzetter, P. 2006, Detection of seismic damage in buildings using time series analysis and pattern recognition, *Proceedings of the 4th World Conference on Structural Control and Monitoring*, San Diego, USA, July 11-13, 1-8, on CD-ROM.

27. De Roeck, G., 2003, The state-of-the-art damage detection by vibration monitoring: the SIMCES experience, *Journal of Structure Control*, 10, 127-134.

28. Doebling, S. W., Farrar, C. R., Prime, M. B. and Shevitz, D. W., 1998, A summary review of vibration-based damage identification methods, *Shock and Vibration Digest*, 30(2), 91-105.

29. Estrada, E., Nazeran, H., Nava, P., Behbehani, K., Burk, J. and Lucas, E., 2004, EEG signal feature extraction for classification of sleep staging, *IEEE-EMBS 2004*, San Francisco CA.196-199.

30. Estrada, E., Nazeran, H., Nava, P., Behbehani, K., Burk, J. and Lucas, E., 2005, Itakura distance: a useful similarity measure between EEG and EOG signals in computer-aided classification of sleep stages, *Proceedings of the 2005 IEEE Engineering in Medicine and Biology 27th Annual Conference*, Shanghai, China, 1189-1192.

31. Fanning, P., and Carden, E. P., 2001, Auto-regressive and statistical process control techniques applied to damage indication in telecommunication masts, *Key Engineering Materials*, 204-205, 251-260.

32. Farrar, C. R. and Worden, K., 2007, An introduction to structural health monitoring, *Royal Society of London Transactions Series A*, 365(1851), 303-315.

33. Fassois, S. D. and Sakellariou, J. S., 2007, Time-series methods for fault detection and identification in vibration structures, *Philosophical Transaction of Royal Society A*, 365, 411-448.

34. Gersch, W. and Sharpe, D. R., 1973, Estimation of power spectra with finite order autoregressive models, *IEEE Transaction on Automatic Control*, 18, 367-369.

35. Gersch, W., Nielsen, N. N., Akaite, H., 1977, Synthesis of multivariate random vibration systems: a two-stage least squares AR-MA model approach, *Journal of Sound and Vibration*, 52(4), 553-565.

36. Gray, Jr., A. H. and Markel, J. D., 1976, Distance measures for speech processing, *IEEE Transaction on Acoustics, Speech, and Signal Processing*, 24(5): 380-391.

37. Haugh, L. D., 1976, Checking the independence of two covariance-stationary time series: a univariate residual cross correlation approach, *Journal of American Statistical Association*, 71, 378-85.

38. He, X. and De Roeck, G., 1997, System identification of mechanical structures by a high-order multivariate autoregressive model, *Computer & Structure*, 64, 341-351.

39. Hong, Y, 1996, Testing for independence between two covariance stationary time series, *Biometrika*, 83(3), 615-625.

40. Huang, C. S., 2001, Structural identification from ambient vibration measurement using the multivariate AR model, *Journal of Sound and Vibration*, 241, 337–359.

41. Humar, J., Bagchi, A. and Xu. H., 2006, Performance of vibration-based techniques for the identification of structural damage, *Structural Health Monitoring*, 5(3), 215-241.

42. Itakura, F., 1975, Minimum prediction residual principle applied to speech recognition, *IEEE Transaction on Acoustics, Speech, and Signal Processing*, 23(1), 67-72.

43. Jones, J. H., 1976, Autoregression order selection, *Geophysics*, 41, 771-773.

44. Kadakal, U. and Yuzugullu, O., 1996, A comparative study on the identification methods for the autoregressive modelling from the ambient vibration records, *Soil dynamics and earthquake engineering*, 15(1), 45-49.

45. Kashyap, R.L., 1980, Inconsistency of the AIC rule for estimating the order of AR models, *IEEE Transaction on Automatic Control*, 25 (5), 283-295.

46. Kong, X., Thakor, N. and Goel, V., 1995, Characterization of the EEG signal changes via Itakura distance, *IEEE-EMBC and CMEC*, 873-874.

47. Kong, X., 1998, Quantification of injury-related EEG signal changes using distance and information measures, Department of Electrical Engineering, Northern Illinois University, DeKalb, IL, Technical report.

48. Kong, X. and Brambrink, A., 1999, Quantification of injury-related EEG signal changes using distance measures, *IEEE Transaction on Biomedical Engineering*, 46(7), 899-901.

49. Ljung, L., 1995, *System Identification: Toolbox − User's Guide*, The Math Works, Natick, MA.

50. Ljung, L., 1999, *System Identification: Theory for the user*s, Prentice Hall, Eaglewood Cliffs, NJ.

51. Lutkepohl, H., 1987, Comparison of criteria for estimating the order of a vector autoregressive process, Journal of Time Series analysis, 6, 35–52.

52. Maple, S. L., 1987, *Digital Spectral Analysis with Applications*, Englewood Cliffs, NJ: Prentice-Hall, Inc.

53. Mattson, S. G. and Pandit, S. M., 2006, Statistical moments of autoregressive model residuals for damage localization, *Mechanical Systems and Signal Processing*, 20(3), 627-745.

54. Mita, A., 2003, *Structural dynamics for health monitoring*, Sankeisha: Japan.

55. Muthuswamy, J. and Thakor, N. V., 1998, Spectral analysis methods for neurological signals, *Journal of Neuroscience Methods*, 83, 1–14.

56. Nair, K. K, Kiremidjian, A. S and Law, K. H., 2006, Time series-based damage detection and localization algorithm with application to the ASCE benchmark structure, *Journal of Sound and Vibration*, 291(1-2), 349-368.

57. Neumaier, A. and Schneider, T., 2001, Estimation of parameters and eigenmodes of multivariate autoregressive models, *ACM Transactions on Mathematical Software*, 27, 27–57.

58. Nuttall, A. H., 1976, Spectral analysis of a univariate process with bad data points via maximum entropy and linear predictive techniques, Technical report 5303, Naval Underwater System Center, New London, CT, USA.

59. Oppenheim, A. V. and Schafer, R. W., 1975, *Digital Signal Processing*, Prentice Hall International, London.

60. Oppenheim, A. V. and Schafer, R. W., 2004, From frequency to quefrency: a history of the cepstrum, *IEEE Signal Processing Magazine*, 21(5), 95-106.

61. Pardoen, G.C., 1983, Ambient vibration test of the Imperial County Services Building, *Bulletin of the Seismological Society of America*, 73, 1895-1902.

62. Pandit, S.M. and Wu, S. M., 2001, *Time Series and System Analysis with Applications*, Krieger, Florida, FL.

63. Pham, T. D. 2006a, LPC cepstral distortion measure for protein sequence comparison, *IEEE Transaction on Nano Bioscience*, 5(2), 83-88.

64. Pham, T. D., Beck, D. and Yan, H., 2006b, Spectral pattern comparison methods for cancer classification based on microarray gene expression data, *IEEE Transaction on Circuits and Systems*, 53(11), 2425-2430.

65. Pham, T. D. 2007, Spectral distortion measures for biological sequence comparisons and database searching, *Pattern Recognition*, 40, 516-529.

66. Pi, Y. L. and Mickleborough, N. C., 1989, Modal identification of vibrating structures using ARMA model. *Journal of Engineering Mechanics*, 115(10), 2232-2249.

67. Priestley, M. B., 1994, *Spectral Analysis and Time Series*, Academic Press, London.

68. Proakis, J. G. and Manolakis, D. G., 2007, *Digital Signal Processing: Principles, Algorithms and Applications*, 4th ed., Pearson Prentice Hall.

69. Pukkila, T. M. and Krishnaiah, P. R., 1988, On the use of autoregressive order determination criteria in univariate white noise tests, *IEEE Transaction on Acoustics, Speech, and Signal Processing*, 36(5), 1396-1403.

70. Rabiner, L. and Juang, B. H., 1993, *Fundamentals of Speech Recognition*, Prentice Hall, ISBN 0-13-015157-2.

71. Rezek, A. and Roberts, S. J., 1997, Parametric model order estimation: a brief review, *Model Based Digital Signal Processing Techniques in the Analysis of Biomedical Signals (Digest No. 1997/009)*, IEE Colloquium,16, 3, 1-3.

72. Rissanen, J., 1978, Modeling by shortest data description, *Automatica*, 14(5), 465–471.

73. Rissanen, J., 1983, A universal prior for integers and estimation by minimum description length, *Annals of Statistics*, 11, 416-431.

74. Schlogl, A., 2006, A comparison of multivariate autoregressive estimators, *Signal Processing*, 86, 2426–2429.

75. Schneider, T. and Neumaier, A., 2001, Algorithm 808: Arfit - a Matlab package for the estimation of parameters and eigenmodes of multivariate autoregressive models, *ACM Transactions on Mathematical Software*, 27, 58−65.

76. Schwarz, G., 1978. Estimating the dimension of a model, *Annals of Statistics*, 6, 461–464.

77. Sohn, H. and Farrar, C. R., 2001, Damage diagnosis using time series analysis of vibration signals, *Smart Materials and Structures*, 10, 446-451.

78. Sohn, H., Farrar, C. R., Hemez, F. M., Shunk, D. D., Stinemates, D. W. and Nadler, B. R., 2003, A review of structural health monitoring literature: 1996-2001, Technical reports, Los Alamos National Laboratory (LANL), LA-13976-MS.

79. Stockham, Jr., T. G., 1972, Image processing in the context of a visual model, *Proceedings of the IEEE*, 60(7), 828-842.

80. Stoica, P. and Moses, R.L., 1997, *Introduction to Spectral Analysis*, Prentice-Hall, Upper Saddle River, NJ.

81. Tohkura, I., 1987, A weighted cepstral distance measure for speech recognition, *IEEE Transaction on Acoustics, Speech, and Signal Processing*, 35(10), 1414-1422.

82. Tong, H., 1977, More on Autoregressive Model Fitting with Noisy Data by Akaike's Information Criterion, *IEEE Transactions on Information Theory*, 409-410.

83. Ulrych, T. J., 1971, Application of homomorphic deconvolution to seismology, *Geophysics*, 36(4), 650–660.

84. Ulrych, T. J. and Bishop, T. N., 1975, Maximum entropy spectral analysis and autoregressive decomposition. *Reviews of Geophysics and Space Physics*, 13(1): 183-200.

85. Van Overschee, P. and De Moor, B., 1993, Subspace algorithms for the stochastic identification problem, *Automatica*, 29, 649-660.

86. Walker, G. T., 1931, On periodicity in series of related terms, *Proceedings of the Royal Society of London. Series A*, 131, 518-532.

87. Wear, K. A., Wagner, R. F. and Gama, B. S., 1995, A comparison of autoregressive spectral estimation algorithms and order determination methods in ultrasonic tissue characterization, *IEEE Transactions on Ultrasonics, Ferroelectrics, and Frequency Control*, 42(4), 709-716.

88. Wei, W. W. S., 1994, *Time Series Analysis*, Addison-Wesley Publishing Co., Inc., Redwood City, CA.

89. Wismer, J., Gearbox analysis using cepstrum analysis and comb liftering, Application note, Bruel & Kjær, Denmark.

90. Worden, K., Manson, G. and Fieller, N. R. J., 2000, Damage detection using outlier analysis, *Journal of Sound and Vibration*, 229(3), 647-667.

91. Worden, K. and Dulieu-Barton, J. M. 2004, An overview of intelligent fault detection in systems and structures, *Structural Health Monitoring*, 3(1), 85-98.

92. Yoshimoto, R., and Mita, A., 2002, Parallel identification of structural damages using vibration modes and sensor characteristics, *JSCE Journal of Structural Engineering*, 48, 487-92.

93. Yule, G. U., 1927, On a method of investigating periodicities in disturbed series with special reference to Wolfer's sunspot numbers, *Philosophical Transactions of the Royal Society of London, Series A.*, 226, 267-298.